Molecular Biology of the Cell
Vol. 20, 4871–4884, December 1, 2009

Caspase-independent Mitochondrial Cell Death Results from Loss of Respiration, Not Cytotoxic Protein Release

Lydia Lartigue,* Yulia Kushnareva,* Youngmo Seong,* Helen Lin,*† Benjamin Faustin,‡ and Donald D. Newmeyer*

*La Jolla Institute for Allergy and Immunology, La Jolla, CA 92037; and ‡The Burnham Institute for Medical Research, La Jolla, CA 92037

Submitted August 3, 2009; Revised September 17, 2009; Accepted September 23, 2009
Monitoring Editor: Thomas D. Fox

In apoptosis, mitochondrial outer membrane permeabilization (MOMP) triggers caspase-dependent death. However, cells undergo clonogenic death even if caspases are blocked. One proposed mechanism involved the release of cytotoxic proteins (e.g., AIF and endoG) from mitochondria. To initiate MOMP directly without side effects, we created a tamoxifen-switchable BimS fusion protein. Surprisingly, even after MOMP, caspase-inhibited cells replicated DNA and divided for ~48 h before undergoing proliferation arrest. AIF and endoG remained in mitochondria. However, cells gradually lost mitochondrial membrane potential and ATP content, and DNA synthesis slowed to a halt by 72 h. These defects resulted from a partial loss of respiratory function, occurring 4–8 h after MOMP, that was not merely due to dispersion of cytochrome c. In particular, Complex I activity was completely lost, and Complex IV activity was reduced by ~70%, whereas Complex II was unaffected. Later, cells exhibited a more profound loss of mitochondrial protein constituents. Thus, under caspase inhibition, MOMP-induced clonogenic death results from a progressive loss of mitochondrial function, rather than the release of cytotoxic proteins from mitochondria.

INTRODUCTION

Apoptosis is an ordered cell death program indispensable for the development and maintenance of multicellular organisms (Horvitz and Sternberg, 1991; Vaux and Korsmeyer, 1999). Apoptotic signaling pathways are engaged by numerous stimuli, including growth factor deprivation, activation of cell-surface death receptors, DNA damage, hypoxia, endoplasmic reticulum (ER) stress, oxidative stress, and cell detachment (anoïkis). Dysfunction of apoptosis pathways can alter the homeostasis of specific cell populations and contribute to pathological conditions as diverse as cancer, diabetes, obesity, ischemia-reperfusion injury, and neurodegeneration (Savill and Fadok, 2000).

Mitochondria were long known as the "powerhouses" of the cell, but more recently have been found to be critical for cell death (Horvitz and Sternberg, 1991; Newmeyer *et al.*, 1994; Brown *et al.*, 1999; Vaux and Korsmeyer, 1999; Wang, 2001). In vertebrates, cell death usually involves a canonical "intrinsic" or mitochondrial apoptotic pathway that depends on mitochondrial outer membrane permeabilization (MOMP) mediated by the proteins Bax and/or Bak (Hsu *et al.*, 1997; Hsu and Youle, 1997; Wolter *et al.*, 1997; Griffiths *et al.*, 1999; Wei *et al.*, 2000, 2001; Antonsson *et al.*, 2001; Kuwana *et al.*, 2002). MOMP allows proteins normally residing in the mitochondrial intermembrane space (IMS) to be released into the cytoplasm. In particular, cytochrome c and Smac/DIABLO trigger activation of the "executioner" caspases-3, -6, and -7, leading to apoptosis (Liu *et al.*, 1996; Nicholson, 1999; Slee *et al.*, 1999; Jiang and Wang, 2000; Acehan *et al.*, 2002; Lavrik *et al.*, 2005; Taylor *et al.*, 2007).

However, executioner caspases are usually not necessary for cell death. Although some investigators proposed that tumor cells can evade apoptosis by preventing executioner caspase activation (Soengas *et al.*, 2001; Liu *et al.*, 2002; Nachmias *et al.*, 2004; Philchenkov *et al.*, 2004; Janssen *et al.*, 2007; Hoffarth *et al.*, 2008), other studies have convincingly shown that MOMP leads to a complete loss of clonogenic survival, even when effector caspases are inactive (Xiang *et al.*, 1996; McCarthy *et al.*, 1997; Amarante-Mendes *et al.*, 1998; Marsden *et al.*, 2006).

Surprisingly, dividing cells can recover after MOMP under the enforced expression of GAPDH (Colell *et al.*, 2007). GAPDH rescues a percentage of cells that have undergone MOMP, allowing them to proliferate. GAPDH thus represents a novel mechanism for cell death regulation downstream of mitochondria. However, because the detailed mechanisms of cell death after MOMP in the absence of caspases are not fully understood, it remains unclear exactly how GAPDH expression allows cells to survive and resume proliferation.

We envisioned two independent mechanisms for caspase-independent cell death after MOMP: first, a gain of death function; or second, a loss of survival function. In the first scenario, mitochondria would release actively cytotoxic IMS proteins such as endonuclease G (endoG) and apoptosis-inducing factor (AIF) into the cytoplasm and nucleus. In the other scenario, key mitochondrial functions (e.g., ATP production) necessary for cell survival would be impaired.

Intriguingly, we found that when caspases were inhibited, MOMP did not provoke an immediate arrest of DNA synthesis or cell proliferation. Rather, cells underwent about

This article was published online ahead of print in *MBC in Press* (http://www.molbiolcell.org/cgi/doi/10.1091/mbc.E09–07–0649) on September 30, 2009.

† Present address: NovaRx, 6828 Nancy Ridge Drive, Suite 100, San Diego, CA 92121.

Address correspondence to: Donald D. Newmeyer (don@liai.org).

two divisions before they arrested. These results do not support a model in which cell death results from the release of cytotoxic proteins from mitochondria. Rather, the data imply a mechanism for MOMP-induced caspase-independent clonogenic cell death in which nuclear DNA synthesis and cell division are inhibited because of a progressive impairment of mitochondrial bioenergetics. Moreover, our results highlight the importance of mitochondrial respiration in cell proliferation, a role that cannot be replaced by glycolysis, despite the well-known shift toward glycolysis, or "Warburg effect" that often occurs in tumors.

MATERIALS AND METHODS

Cell Lines and Reagents

Parental 293T cells (human embryonic kidney epithelial cells) and 293T cells stably expressing murine BimS-ER protein were grown in Dulbecco's MEM medium (Invitrogen, Carlsbad, CA) supplemented with 10% of charcoal-treated fetal bovine serum (Hyclone, Logan, UT) and antibiotics at 37°C in a humidified CO_2 incubator. Stable cell lines were generated by transfecting (Lipofectamine 2000, Invitrogen) parental 293T cells with pIres2-EGFP-BimS-ER, pIres2-EGFP-BimSG68E-ER, or pIres2-mtDsRed2-BimS-ER and selected with 1 mg/ml G418. 4-Hydrotamoxifen (OHT, Sigma, St. Louis, MO) was used to induce cell death at 0.2–1 μM. Z-Val-Ala-Asp(OMe)-FMK and Q-Val-Asp-OPh (MP Biomedicals, Solon, OH) were used at 100 and 20 μM, respectively. Both caspase inhibitors were added to the cells 1 h before OHT treatment. Oligomycin and rotenone were purchased from Sigma; CCCP was provided in the Mitoprobe $DilC_1$ (5) Assay Kit from Molecular Probes (Eugene, OR).

Generation of Expression Constructs

The cDNA encoding the BimSG68E-ER mutated protein was generated with the QuickChange Site-directed Mutagenesis Kit (Stratagene. La Jolla, CA) by using the following primers: (forward) 5′-GAG CTG CGG CGG ATC GAA GAC GAG TTC AAC GAA-3′ and (reverse) 5′-TTC GTT GAA CTC GTC TTC GAT CCG CCG CAG CTC-3′ and pIres-EGFP2-BimS/ER as a template.

Determination of Bax Activation

The activation of the proapoptotic protein Bax was analyzed by flow cytometry after immunostaining of cells in suspension. The cells were harvested by centrifugation (800 × *g*, 5 min) and resuspended in 850 μl of PBS before the addition of 150 μl of 2% formaldehyde. After an incubation at 4°C for 50 min under agitation, fixed cells were permeabilized in 1 ml of PBS containing 0.2% Tween-20 for 15 min at 37°C, spun down, and bound with primary antibody Bax-N20 (Santa Cruz Biotechnology, Santa Cruz, CA) overnight at 4°C. Cells were then washed twice in PBS containing 0.2% Tween-20 and incubated with Texas Red–conjugated rabbit secondary antibody (Amersham Biosciences, Piscataway, NJ) for 1 h at 4°C. Measurements were done on the FL2 detector after two more washes in PBS containing 0.2% Tween-20.

Cellular Fractionation and Western Blot Analysis

Isolation of the mitochondrial and cytosolic fractions was performed as previously described (Kluck *et al.*, 2000). Briefly, 10^8 cells were harvested and washed twice in PBS before washing in lysis buffer (250 mM sucrose, 20 mM HEPES/KOH, pH 7.5, 50 mM KCl, 2.5 mM $MgCl_2$, 1 mM DTT, 5 μg/ml cytochalasin B, 1 μg/ml cycloheximide, and a tablet of Complete protease inhibitor mixture; Roche, Indianapolis, IN). After centrifugation, the pellet was resuspended in an equal volume of lysis buffer and placed on ice for 30 min. The cells were then homogenized with a Potter-Elvehjem Teflon-coated pestle (50–100 strokes) until 50% of them became permeable to trypan blue and immediately spun down twice for 5 min at 300 × *g* to remove nonlysed cells and nuclei. A final centrifugation at 15,000 × *g* for 15 min separated cytosol (supernatant) from the heavy membrane pellet, containing mitochondria. The pellet was resuspended in a volume equal to the supernatant volume before protein quantification (Bradford assay) and Western blot. Equivalent aliquots of cytosol and mitochondrial extracts were loaded on 12% SDS-polyacrylamide gels. Western blot were probed with murine anti-cytochrome c (clone 7H8.2C12, BD-PharMingen, San Diego, CA) or anti-VDAC (Calbiochem, La Jolla, CA) antibodies followed by horseradish peroxidase–conjugated anti-mouse antibody (Amersham Pharmacia Biotech, Piscataway, NJ) and developed with enhanced chemiluminescence kit (Amersham Pharmacia Biotech).

Immunofluorescence and Confocal Microscopy

293T cells stably transfected with pIres2-EGFP-BimS-ER were seeded in four-well Lab-Tek II Chambered coverglass slides (Rochester, NY) 24 h before the addition of 100 μM zVAD-fmk and 1 μM of OHT. Eight hours after the different treatments, cells were fixed in 3.7% formaldehyde for 20 min, washed in PBS, and permeabilized with 0.5% Triton X-100. Nonspecific binding was blocked by incubating cells in 0.2% gelatin/PBS for 30 min. Staining was performed using a primary antibody against cytochrome c (clone 6H2.B4, BD-PharMingen), HtrA2/Omi (R&D Systems, Minneapolis, MN), OxPhos Complex IV subunit II (Molecular Probes), Hsp60 (Santa Cruz Biotechnology), AIF (Santa Cruz Biotechnology), endoG (ProSci Incorporated, Poway, CA), and a fluorescent secondary antibody conjugate, AlexaFluor 568 or 647 goat anti-mouse or rabbit IgG, (Molecular Probes). Images were acquired using a Nikon Eclipse TE 300 microscope (Melville, NY) coupled to a Bio-Rad MRC 1024 confocal head and a 15 mW krypton/argon laser unit (Richmond, CA). Intracellular localization of the different proteins was individually detected by using a 488-nm (green fluorescent protein [GFP]), 568-nm (AlexaFluor 568) or 647-nm (AlexaFluor 647) excitation line from the laser attenuated at 95% and a 522DF35 (GFP), 605DF32 (AlexaFluor 568), or 680DF32 (AlexaFluor 647) emission filter. Mitotracker Red CMXRos (Molecular Probes) was used to evaluate the mitochondrial transmembrane potential on fixed cells by microscopy. Images were taken with a 40× oil immersion objective and acquired using Lasersharp 2000 software (Bio-Rad). For each experiment (n = 2–3), at least 500 cells were counted for each sample.

Determination of Cell Death by Flow Cytometry

Mitochondrial membrane potential ($\Delta\Psi_m$) was measured with tetramethylrhodamine ethyl ester, TMRE (Molecular Probes). Presence of phosphatidylserine on surfaces of apoptotic cells was followed using recombinant human annexin V (Caltag, Burlingame, CA). Briefly, adherent 293T cells were detached by short treatment with trypsin-EDTA, collected 1) in 200 μl of prewarmed PBS supplemented with 200 nM of TMRE or 2) in 200 μl of annexinV-binding buffer supplemented with 2 μl of recombinant annexin V–adenomatous polyposis coli (APC) and incubated 20 min at 37°C or 10 min at room temperature, respectively, before measurement by flow cytometry. Cells were excited by an air-cooled argon 488-nm laser, and the signals from TMRE and annexinV-APC were detected on the FL2 and FL4 detectors, respectively. The data obtained were acquired using CellQuest software (BD FACS Systems, Sunnyvale, CA) and analyzed using FlowJo software (Tree Star, Ashland, OR).

Analysis of DNA Synthesis

Cells entering and progressing through S phase of the cell cycle were detected using the APC bromodeoxyuridine (BrdU)/7–aminoactinomycin D (7-AAD) Flow kit (BD-PharMingen) according to the manufacturer's instructions. More precisely, the cells were incubated with a solution of BrdU (10 μM) for 60 min before fixation and permeabilization with appropriate buffers. The newly incorporated BrdU was then immunostained with an APC-coupled anti-BrdU antibody. 7-AAD was added for 20 min before measurement to analyze cell cycle distribution. Analyses were done by flow cytometry through FL2 (7-AAD) and FL4 (BrdU) detectors. For each time point of kinetic experiments, BrdU solution was added to cell culture for the last 45 min of death induction.

Cell Proliferation Studies

Cell division was followed using carboxyfluorescein diacetate succinimidyl ester (CFSE; Molecular Probes) dye (Lyons *et al.*, 2001). 293T cells stably expressing mtDsRed2/BimS-ER were trypsinized, spun down, and resuspended at 10^6 cells/ml in a solution of BSA in 0.1% PBS, containing CFSE dye at a final concentration of 6.25 μM. The staining was stopped after 10 min by addition of an equal volume of FBS. The cells were then washed twice and seeded in 12-well plates at 10^5 cells/well. Cell division was analyzed every 24 h by flow cytometry with detection of green fluorescence (CFSE) in the FL1 channel and red fluorescence (mtDsRed2) in FL2.

Oxygen Consumption and ATP Assays

Oxygen consumption was measured using a Clark-type electrode (Oxygraph, Hansatech Instruments, King's Lynn, Norfolk, United Kingdom). The cells ($8–10 \times 10^6$) were pelleted at 200 × *g* (2 min) and resuspended in 0.7–0.8 ml glucose-containing DMEM. After recording basal respiration for 2–3 min, oligomycin (1.25 mg/ml) was added, followed by sequential additions of FCCP (50–100 nM) until the respiration rate reached maximum. For respiration measurements in digitonin-permeabilized cells, the cells ($8–10 \times 10^6$) were resuspended in 0.7–0.8 ml sucrose-based medium containing 250 mM sucrose, 2 mM KH_2PO_4, 10 mM HEPES (pH 7.4), 2 mM $MgCl_2$, 40 μM EGTA, and 5 mM glutamate plus 5 mM malate as Complex I substrates. In some experiments, glutamate and malate were replaced with 5 mM succinate (in the presence 0.5 μM rotenone) as a Complex II substrate. In experiments with exogenously added cytochrome c, $MgCl_2$ was omitted from the medium. The plasma membrane was permeabilized by addition of a titrated amount of digitonin (0.006%). ADP (800 μM), oligomycin, and FCCP were added as indicated on the figures. In control cells, mitochondria were functionally intact as indicated by the respiratory control ratio (RCR) of >6. The high RCR confirms that digitonin, at the concentration used, did not compromise mitochondrial membrane integrity. Respiration rates were normalized per equal numbers of live cells, evaluated by Trypan Blue exclusion.

ATP assays were performed using the CellTiter-Glo Luminescent Cell Viability Assay kit (Promega, Madison, WI) following the manufacturer's instructions. Briefly, 5000 cells were seeded in each well of a 96-well plate and treated with vehicle, zVAD-fmk, or OHT plus zVAD-fmk in a final volume of 100 μl. After 8, 24, 48, or 72 h of treatment, an equal volume of CellTiter-Glo Reagent (Promega) was added to the well and incubated for 10 min at room temperature under agitation, before measurement using a SpectraMax luminescence microplate reader. The ATP levels were calculated from an ATP standard curve performed at the same time and normalized to the control sample at each time point. Each measurement was done in triplicate and the experiment was repeated three times.

Determination of Respiratory Complex Enzymatic Activity

Respiratory complex activities were analyzed using mitochondria isolated from cells (as described above). Pellets were conserved at −80°C until used. Assays were carried out in 384-well plates using a Molecular Devices M5 spectrophotometer(Sunnyvale, CA) and standardized reproducible methods as described previously (Aleardi *et al.*, 2005). Complex I (NADH:Ubiquinone Reductase): The oxidation of NADH by complex I was recorded using the ubiquinone analogue decylubiquinone as electron acceptor (Birch-Machin *et al.*, 1989). The basic assay medium (35 mM KH_2PO_4, 5 mM $MgCl_2$, and 2 mM KCN, pH 7.2) was supplemented with defatted BSA (2.5 mg/ml), antimycin A (2 μg/ml), 65 mM decylubiquinone, and 10 mM NADH in a final volume of 100 μl. The enzyme activity was measured by starting the reaction with 5 μg of mitochondrial protein. The decrease in absorption due to NADH oxidation was measured at 340 nm at 30°C both in the absence and in the presence of 10 μg/ml rotenone. Complex II (succinate dehydrogenase): The assay was performed by following the decrease in absorbance at 600 nm at 37°C resulting from the reduction of 2,6-dichlorophenolindo-phenol in 100 μl of medium containing 51 mM KH_2PO_4 (pH 7.4), 3 mM KCN, 20 μg/ml rotenone, 20 mM succinate, and 1 μg mitochondrial protein. The reaction was initiated by the addition of 1.3 mM phenazine methasulfate and 0.18 mM 2,6-dichloroindophenol sodium salt hydrate. Complex IV (cytochrome c-oxidase): The oxidation of cytochrome c was monitored at 550 nm at 37°C according to the method originally described in Wharton and Tzagoloff (1967). Cytochrome c oxidase activity was measured as the decrease of 90% reduced cytochrome (50 μM) in a final volume of 100 μl in the presence of 2 μg mitochondrial proteins with or without 0.2 mM KCN. Citrate synthase: The reduction of 5,5-dithiobis(2-nitrobenzoic acid) by citrate synthase at 412 nm was followed in a coupled reaction with acetyl CoA and oxaloacetate. A reaction mixture of 20 mM Tris·HCl, pH 8.0, 0.1 mM acetyl-CoA, 0.1 mM 5,5-dithiobis(2-nitrobenzoic acid), and 5 μg mitochondrial proteins was incubated at 37°C for 5 min. The reaction was initiated by the addition of 0.5 mM oxaloacetate.

Amplification of Mitochondrial and Nuclear DNA from Whole Cells

Mitochondrial and nuclear DNA were amplified as described (Milano and Day, 2000). Briefly, 2×10^6 cells were seeded in 10-cm Petri dishes, treated as indicated for 8 or 24 h, and harvested. After two washes in a large volume of PBS, pellets were finally put in suspension into 100–200 μl of PBS and counted in triplicate using a ViCell automated cell counter (Beckman Coulter, Fullerton, CA). Each sample was then diluted to 2×10^3 cells/ml in PBS and 1 μl was used for the PCR reaction. Templates were preheated for 5 min at 99.9°C in presence of 10× enzymatic buffer and dH_2O, and kept on ice for a few minutes. Then, a mixture containing the primers (mtDNA or nDNA), dNTP, $MgCl_2$ and Amplitaq Gold DNA polymerase (Applied Biosystems) was added, and the PCR program was performed as follows: preincubation at 95°C for 10 min; 22 or 25 cycles of 94°C for 45 s, 50°C for 30 s, and 72°C for 1 min; and 72°C for 10 min, and keep at 4°C. Primers pairs used to amplify a fragment of the human mitochondrial or nuclear genome were, respectively, denoted mtDNA (forward primer/mt2981: 5′-ACG ACC TCG ATG TTG GAT C-3′ and reverse primer/mt3245: 5′-GCT CTG CCA TCT TAA CAA ACC-3′), and n-DNA (forward primer/28S rRNA-7358: 5′-TTA AGG TAG CCA AAT GCC TCG-3′ and reverse primer/28S rRNA-7460: 5′-CCT TGG CTG TGG TTT CGC T-3′). Mt-DNA and n-DNA primers sets give rise in theory to a PCR product of 264 and 102 base pairs, respectively. The amplification of the endogenous control 28S rRNA (n-DNA primer pair) was used to standardize the mitochondrial content by comparative analysis. For a control, H_2O_2 was used as a mtDNA-damaging agent known to induce loss of mtDNA (Cha *et al.*, 2005).

RESULTS

Activation of a BimS-ER Fusion Protein Induced the Mitochondrial (Intrinsic) Pathway of Apoptosis

To trigger MOMP "surgically" without inducing other nonspecific apoptotic signaling pathways, we used a molecular switch consisting of a fusion of the proapoptotic BH3-only protein BimS to a OHT-responsive domain of the ER (Figure 1A). We stably transfected 293T human embryonic kidney cells with the BimS-ER gene linked via an internal ribosome entry site (IRES) to GFP or a mitochondria-targeted DsRed protein. We used fluorescence-activated cell sorting (FACS) to enrich for cells expressing relatively high levels of BimS-ER.

BimS can directly induce Bax-dependent MOMP (Kuwana *et al.*, 2005). As expected, at 6 h after OHT addition, a majority of the cells expressing BimS-ER exhibited apoptotic morphology. These cells were positive for Annexin V, contained activated Bax, and had undergone MOMP, as evidenced by the dispersal of cytochrome c throughout the cell (Figure 1). We were never able to obtain stable BimS-ER transfectant 293T cultures that underwent a percentage of OHT-inducible cell death higher than ~80%, nor any HeLa cells stably expressing BimS-ER. Probably BimS-ER is "leaky," supplying a weak death signal even in the absence of OHT, and if so, cells may not readily tolerate this protein.

Loss of $\Delta\Psi_m$ is an early caspase-dependent consequence of MOMP (Kluck *et al.*, 1997; Bossy-Wetzel *et al.*, 1998; Waterhouse *et al.*, 2001; Ricci *et al.*, 2004). We observed a loss of $\Delta\Psi_m$ as early as 2 h after OHT addition in cells not treated with caspase inhibitors (Figure 1E). However, the pan-caspase inhibitor zVAD-fmk blocked this early $\Delta\Psi_m$ loss (Figure 1G). Very few of the parental cells, or control cells stably expressing a mutant BimS(G68E)-ER with greatly reduced proapoptotic activity (Marani *et al.*, 2002; Figure 1A), exhibited a loss of $\Delta\Psi_m$ or any other signs of cell death, with or without added OHT (Figure 1, B–G). All of these data are consistent with a specific and fairly rapid induction of the canonical "intrinsic" pathway of cell death.

In the Absence of Caspase Activation, "Pure" MOMP Had No Immediate Repercussions on DNA Synthesis and Cell Proliferation

To assess effects of MOMP on nuclear function, we measured DNA synthesis by BrdU pulse-labeling at various times after OHT treatment. Flow cytometry showed that both DNA content and BrdU incorporation were strongly reduced after OHT treatment alone, simply due to apoptotic DNA fragmentation (Figure 2A). However, zVAD-fmk blocked this DNA fragmentation, allowing us to observe the effects of MOMP per se on DNA synthesis and cell cycle profile. Surprisingly, the percentage of S-phase cells and the rate of BrdU incorporation remained unchanged for 24 h (Figure 2A), although at least 37% of the cells had undergone MOMP in this experiment (not shown). Only at ~48 h after OHT addition did we detect a subpopulation of cells with reduced BrdU incorporation during the 1-h pulse and hence a slower rate of DNA synthesis (Figure 2B, arrows). At 72 h, this population became almost BrdU-negative, implying a virtual halt in DNA replication. To confirm that this cell population represented the portion that had earlier undergone MOMP, we analyzed single cells (Figure 2C) simultaneously for BrdU incorporation and HtrA2/Omi release (as a marker for MOMP.) Consistent with the flow cytometry data, a loss of replication was seen only after ~2 d. At 48 and 72 h, only 28.4 and 17%, respectively, of the Omi-diffuse cells were BrdU-positive, compared with 45.7% at 24 h. Moreover, the BrdU fluorescence in these S-phase cells was reduced in intensity. Thus, cells that had undergone MOMP replicated DNA at normal rates for at least 24 h, but later more and more slowly, until DNA synthesis came to a virtual halt by 72 h.

To determine whether cells might even be able to divide after undergoing MOMP, we labeled the plasma membranes of 293T BimS-ER cells with the viable fluorescent dye CFSE.

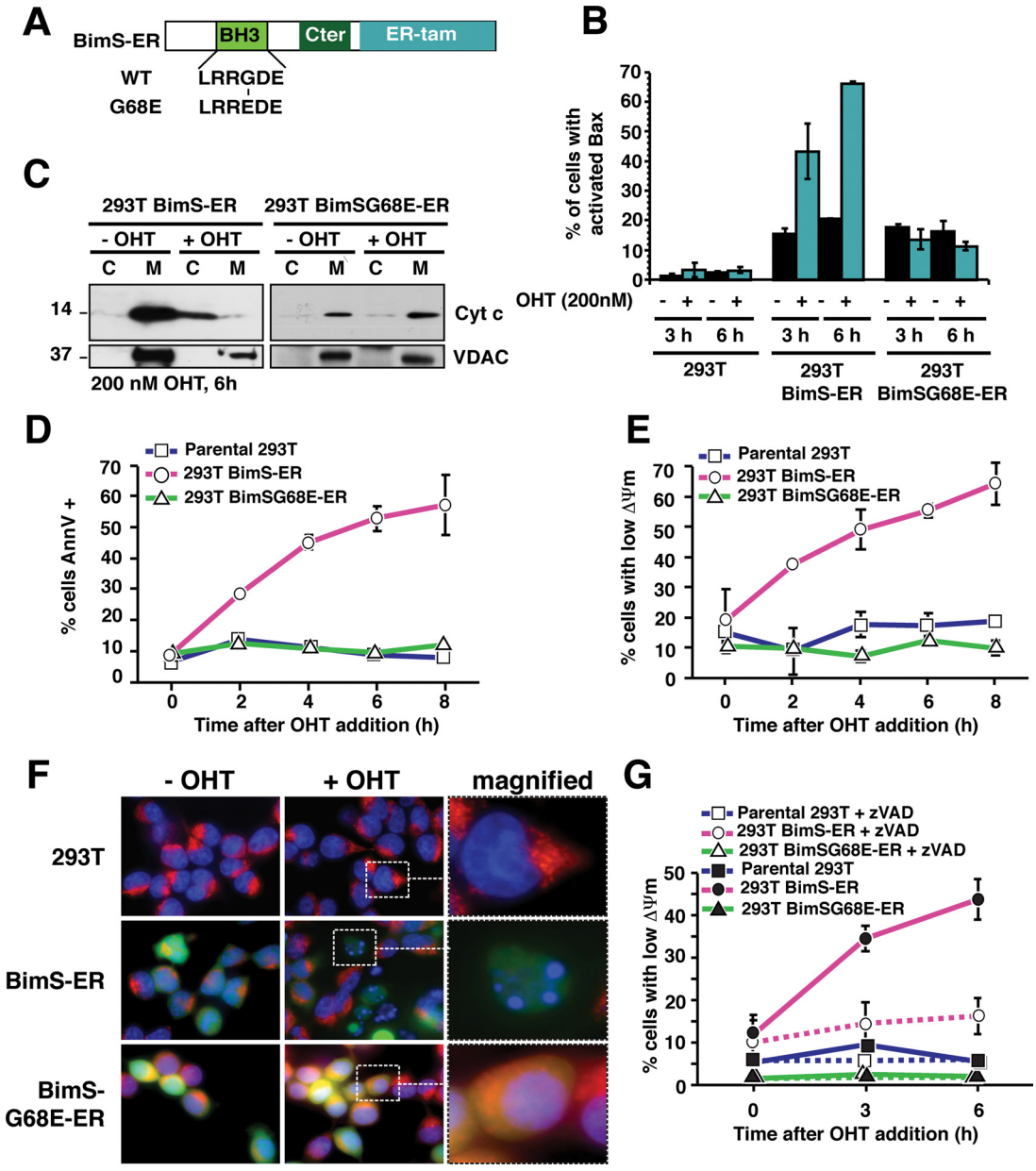

Figure 1. BimS-ER activation induced the mitochondrial pathway of apoptosis. Parental 293T and 293T cells stably expressing BimS-ER/GFP or BimSG68E-ER/GFP were treated with 200 nM of 4-hydroxytamoxifen (OHT). (A) Schematic representation of BimS-ER fusion protein. Shown are the BH3 domain, the C-terminal region of BimS (Cter), and the tamoxifen-binding region of the estrogen receptor (ER-tam). (B) Expression of WT but not G68E mutant BimS-ER confers the ability of OHT to induce Bax activation in 293T cells. Cells with cultured with or without OHT for the indicated times, and Bax activation was monitored by flow cytometry using an antibody (N20) specific for activated Bax. (C) WT, but not G68E, BimS-ER induces cytochrome c release. Cells were cultured for 6 h with or without OHT, then the cytosolic and mitochondrial fractions were analyzed for cytochrome c by immunoblot. (D and E) WT but not mutant BimS-ER induces hallmarks of apoptosis: PS externalization and mitochondrial depolarization. Parental 293T and derivatives stably expressing BimS-ER/GFP or the BH3-domain mutant BimS(G68E)-ER/GFP were treated with OHT or vehicle for the times indicated. Flow cytometry was used to assess the percentage of cells either positive for binding of annexinV (D) or negative for staining with TMRE (E). (F) WT but not mutant BimS-ER induces apoptotic DNA morphology and loss of mitochondrial $\Delta\Psi_m$ (TMRE staining) as seen by laser confocal microscopy. Parental, BimS-ER/GFP or BimS(G68E)-ER/GFP 293T cells were incubated in the presence of OHT for 6 h and stained with both Hoechst 33258 (1 mg/ml) and TMRE (200 nM) for 10 and 20 min, respectively, at 37°C. Images were acquired using Zeiss Axiovert 200 imaging station. (G) Time course of caspase-dependent mitochondrial depolarization. 293T cells stably expressing BimS-ER or BimS(G68E)-ER were cultured with or without 200 nM of OHT and with or without caspase inhibitor zVAD-fmk (100 μM) for 3 or 6 h. TMRE retention ($\Delta\Psi_m$) was analyzed by flow cytometry. Error bars, SD from three independent experiments.

CFSE partitions equally to the daughter cells at each cell division, and thus the fluorescence in each cell is halved. Intriguingly, in the presence of caspase inhibitor (zVAD-fmk or Q-VD), cells underwent about two rounds of division after MOMP (Figure 2D). Only after ~48 h did a subpopulation of the cells succumb to cell cycle delay or arrest. This was seen as a splitting of the CFSE fluorescence histogram into two peaks: one that maintained higher CFSE fluores-

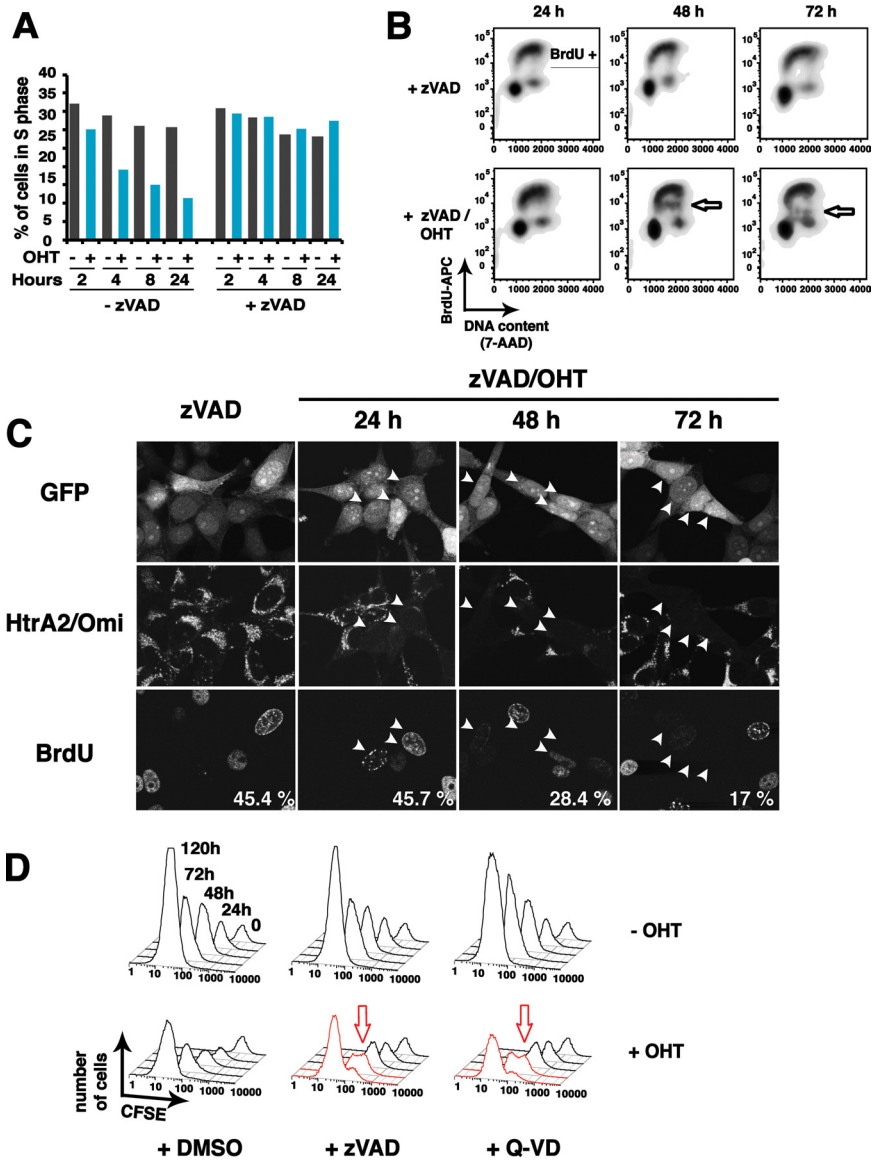

Figure 2. DNA synthesis and cell division continued during the first 48 h after BimS-ER activation, but then slowed. (A) DNA synthesis rate and cell cycle distribution were unaffected for the first 24 h. 293T cells stably expressing BimS-ER were cultured for the indicated times with or without 1 μM of OHT in presence or absence of 100 μM of zVAD-fmk. BrdU (10 μM) was added to the cells for the last hour of death induction. The percentage of cells in S phase in the whole population was then determined using an APC-conjugated anti-BrdU antibody by flow cytometry. (B) A subpopulation of cells exhibited gradually declining rates of DNA synthesis from 48 to 72 h after BimS-ER activation. Cells were treated as in A. Flow cytometry was used to measure BrdU incorporation versus total DNA content (cell cycle phase) in individual cells following OHT addition. The arrows mark a portion of the cells displaying a gradually declining rate of BrdU incorporation (DNA synthesis) throughout S phase. (C) Laser confocal microscopy confirmed that cells in which Htra2/Omi had been released from mitochondria (i.e., cells having undergone MOMP) were the same cells that displayed reduced BrdU incorporation at later time points. The assay was performed as in B, but after fixation, cells were costained for BrdU and HtrA2/Omi. (D) A subpopulation of cells underwent a delayed proliferative arrest ~48 h after BimS-ER activation. 293T cells stably expressing BimS-ER/mtDsRed2 were stained with the stable plasma-membrane–associating dye CFSE and treated with vehicle or 1 μM of OHT in the presence or absence of zVAD-fmk or Q-VD for the times indicated. At each successive time point, CFSE fluorescence intensity was reduced, consistent with cell division, except in a portion of the cells indicated by red arrows, whose cytokinesis was evidently arrested or delayed.

cence and thus failed to divide (arrow in Figure 2D) and another CFSE low peak of dividing cells. These were the OHT-resistant survivors, which eventually outgrew the arrested cells. The cells failing to divide at 48–72 h were likely those that had undergone MOMP and exhibited lower BrdU incorporation in single-cell analysis (Figure 2C). In this particular experiment, OHT treatment (without caspase inhibitor) induced apoptosis in ~50% of the cells.

In the Absence of Caspase Activation, MOMP Did Not Trigger the Release of AIF and endoG from Mitochondria

As discussed above, MOMP could theoretically induce a gain of death function through the release of cytotoxic molecules from mitochondria, such as AIF and endoG. Others have proposed that these proteins could act in a caspase-independent cytotoxic manner by translocating to the nucleus and inducing DNA fragmentation and chromatin condensation (Susin *et al.*, 1999; Li *et al.*, 2001). However, we observed that neither AIF (Figure 3A) nor endoG (Figure 3B) was released from mitochondria 24 h after OHT treatment, whereas cytochrome c was dispersed into the cytoplasm. These results are consistent with earlier observations that the release of AIF and endoG is caspase-dependent (Arnoult *et al.*, 2003). Thus, it is unlikely that the proliferation arrest observed 48 h after MOMP was caused by these mitochondrial proteins.

In the Absence of Caspase Activation, MOMP Led to a Loss of Mitochondrial Function

An alternative hypothesis is that MOMP leads to a loss of essential mitochondrial functions. Earlier studies showed that caspase inhibition prevents the early loss of $\Delta\Psi_m$ after MOMP induced by several apoptosis-inducing agents (Bossy-Wetzel *et al.*, 1998; von Ahsen *et al.*, 2000; Waterhouse *et al.*, 2001; Ricci *et al.*, 2004). It appears that initially after MOMP, although cytochrome c is dispersed throughout the cell, this protein is present in sufficient concentrations to support respiration and the maintenance of $\Delta\Psi_m$. However, the long-term repercussions of MOMP have not been thoroughly examined. We therefore monitored $\Delta\Psi_m$ for 72 h (Figure 4A). Caspase inhibition did at first prevent loss of $\Delta\Psi_m$, as previously reported. However, by 24 h after OHT

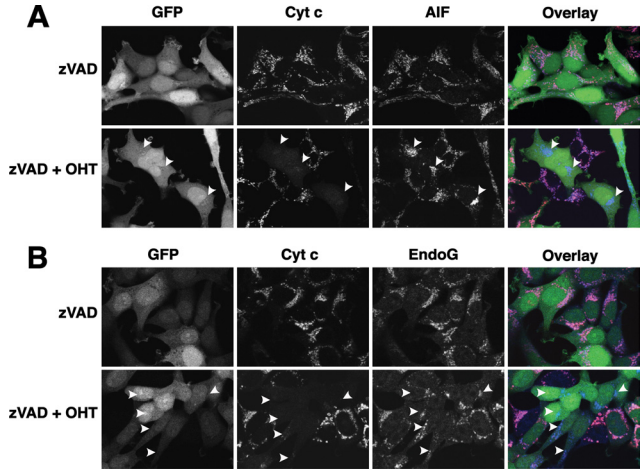

Figure 3. BimS-ER-induced MOMP did not trigger the release of AIF and endoG from mitochondria concomitantly with release of cytochrome c. BimS-ER/GFP–expressing cells were cultured with or without OHT in the presence or absence of zVAD-fmk for 24 h. (A) Lack of concomitant release of AIF with cytochrome c. In overlay images, green, red, and blue colors represent, respectively, the distributions of GFP, cytochrome c, and AIF. (B) Lack of concomitant release of endoG with cytochrome c. In overlay images, green, red, and blue colors represent, respectively, the distributions of GFP, cytochrome c, and endoG.

addition, more than half of the cells that had undergone MOMP also lost $\Delta\Psi_m$, and by 72 h, 80% had lost $\Delta\Psi_m$. Similar results were obtained with Q-VD instead of zVAD-fmk (not shown), and we previously observed a similar gradual loss of $\Delta\Psi_m$ in HeLa cells treated with actinomycin D in the presence of Q-VD (Colell *et al.*, 2007).

Similarly, cellular ATP content remained high for at least 8 h after OHT addition (Figure 4B), but at 24 h, ATP was reduced 50%. Nevertheless, these cells were able to synthesize DNA and divide like untreated cells. However, by 72 h after MOMP, ATP was nearly depleted (Figure 4B), cells had stopped dividing (Figure 2D), and BrdU incorporation was barely detectable (Figure 2B). Because this near-depletion in ATP coincided with cell cycle arrest/delay and because ATP and other nucleoside triphosphates (NTPs) are of course essential for DNA synthesis, we hypothesize that ATP depletion is a direct cause of proliferative slowdown in these cells. Supporting this idea, we saw that chemical inhibitors of mitochondrial OxPhos (but not glycolysis) caused a profound block in cellular proliferation (see Figure 8).

In the Absence of Caspase Activation, MOMP Leads to an Impairment of Respiratory Activity within 4–8 h

More than 50% of the cells with permeabilized MOMs still contained Hsp60, a mitochondrial matrix protein, at 72 h (see Figure 7B), a time when nearly all cells that had undergone MOMP were depleted of ATP and had ceased DNA synthesis and cell division. Thus, mitochondria were still present in these cells, although their clustering made it impossible to discern individual organelles by confocal microscopy. Given this persistence of mitochondria, we asked whether autophagy was induced after BimS-ER-induced MOMP under caspase inhibition. Autophagy is typically accompanied by the conversion of LC3-I (microtubule-associated protein 1 light chain 3; 18 kDa) into the active form LC3-II (16 kDa; Supplemental Figure S1B). The LC3-II band was not enhanced in cells treated with OHT plus zVAD-fmk, but did increase markedly in control cells treated with rapamycin to induce autophagy. Moreover, the addition of wortmannin or 3-methyladenine, two autophagy inhibitors, had no effect on cell proliferation or delayed arrest after treatment with OHT plus zVAD-fmk (data not shown). We conclude that autophagy was not increased as a result of MOMP in these cells.

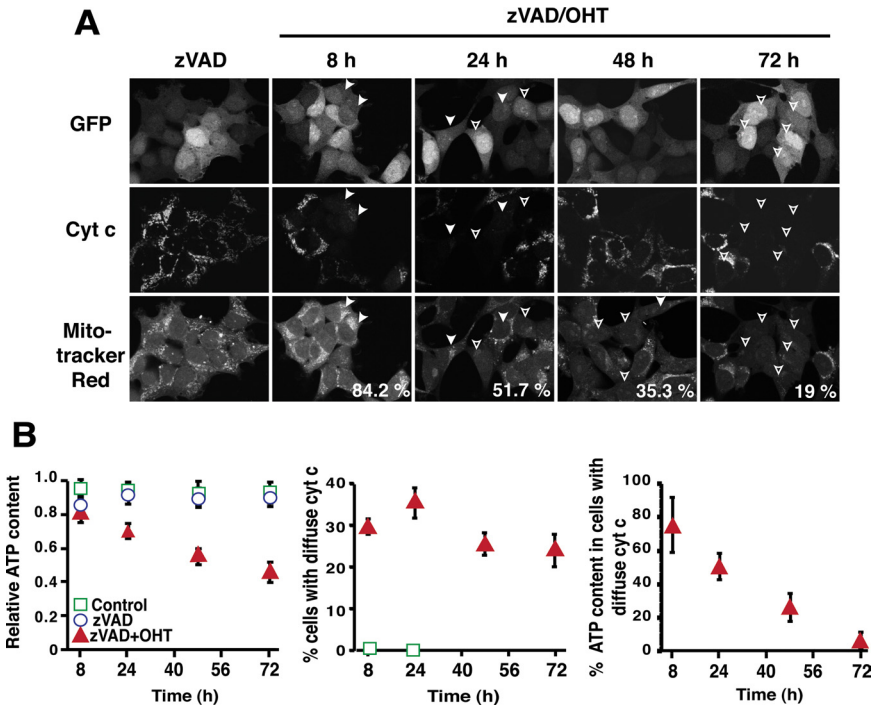

Figure 4. BimS-ER-induced MOMP led to a gradual loss of mitochondrial polarization and cellular ATP content. 293T cells stably expressing BimS-ER/GFP were cultured with or without OHT in the presence of zVAD-fmk for the times indicated. (A) An increasing number of cells lost mitochondrial membrane potential ($\Delta\Psi_m$) over the course of 72 h after BimS-ER activation. Of the cells that had released cytochrome c, the percentage that retained TMRE staining, i.e., that were $\Delta\Psi_m^+$, is indicated at the bottom right corners of the lower panels. (B). A steady decline of cellular ATP content after MOMP culminated in near depletion of ATP at 72 h. Left panel, ATP content in the bulk cell population, including cells that had not undergone MOMP. ATP content was determined in each sample by bioluminescence. Error bars, SD from three independent experiments each done in triplicate. Middle panel, percentage of cells that had undergone MOMP (cytochrome c release) at various times. At the indicated times after OHT addition, cells were fixed and immunostained for cytochrome c. More than 500 hundred cells were counted in each case (n = 2). Right panel, the percentages obtained in the middle panel were used to calculate the ATP content of cells that had undergone MOMP, based on the assumption that the cells that failed to release cytochrome c did not lose any ATP content.

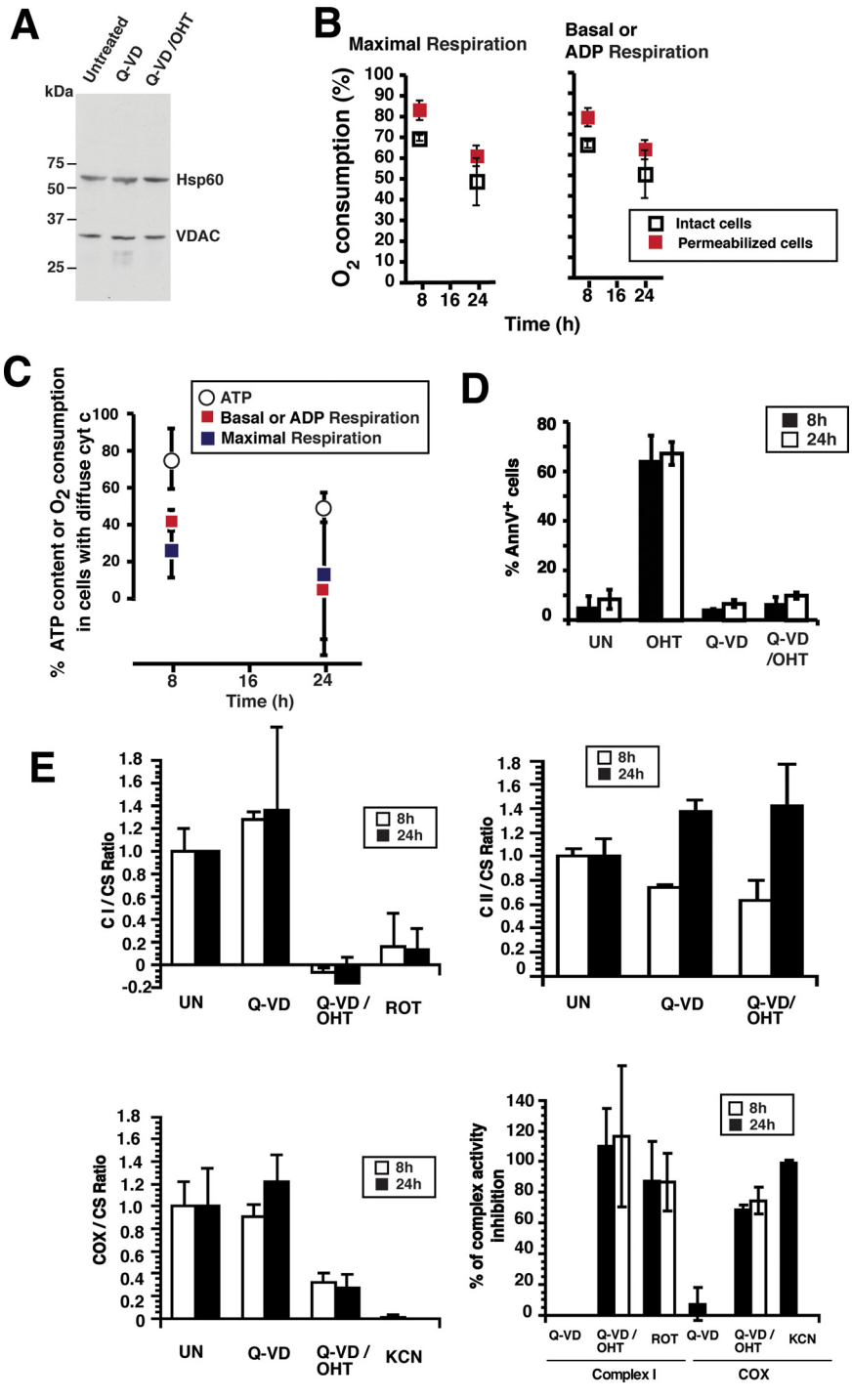

Figure 5. BimS-ER-induced MOMP leads to an early, but not immediate, loss of respiratory function. (A) Cellular amounts of mitochondrial proteins VDAC and Hsp60 remained constant for 24 h. Mitochondria were isolated from 293T cells stably expressing BimS-ER, untreated, or treated with OHT in the presence or absence of Q-VD for 24 h, and then immunoblots were probed with antibodies to VDAC or mitochondrial Hsp60. An amount of mitochondrial fraction corresponding to the same equivalent number of cells was loaded in each lane. (B) BimS-ER–expressing cell populations displayed a gradual loss of respiration after OHT addition. Respiratory rates were determined by polarography either in intact or digitonin-permeabilized cells, as indicated. Right panel, basal respiration (intact cells) or ADP-stimulated respiration (permeabilized cells); left panel, the maximal respiration after FCCP addition. Error bars, SD from three independent experiments. Note that these measurements were made with mixed live/dead cell populations, and thus these values represent an overestimate of the respiratory capacity of cells that underwent MOMP. (C) A strong and rapid decline of respiration rate follows MOMP. The percentages obtained in B were used to calculate the percentage of respiration rate remaining in cells that had undergone MOMP, based on the assumption that the cells that failed to release cytochrome c maintain their respiratory functions intact. For comparison, ATP levels from the same experiment (Figure 4B), corrected in a similar way for the percentage of cells undergoing MOMP, were included. Note that loss of respiration preceded ATP depletion. (D) A separate experiment evaluated the loss of activity of individual respiratory complexes (RCs). Shown is the percentage of apoptotic cells in this experiment, as measured by annexin V staining 8 and 24 h after OHT addition in presence or absence of Q-VD. (E) For the same experiment as shown in D, activities of Complex I, CI (top left), Complex II, CII (top right), and cytochrome c oxidase, COX (bottom left) activity on mitochondria isolated from 293T cells stably expressing BimS-ER treated or not with OHT in presence or absence of Q-VD for 8 and 24 h. Values were normalized to citrate synthase activity (CS), whose activity is not affected by the different treatments. Rotenone and potassium cyanide (KCN), specific inhibitors of CI and COX, respectively, were used as controls. The percentage of CI and COX activity inhibition was calculated compared with untreated samples and is presented in the bottom right panel. Note that MOMP in the presence of caspase inhibitor caused the loss of nearly all Complex I even as early as 8 h; ~50% of COX activity was lost by 8 h, and this was unchanged at 24h, and Complex II activity was unaffected.

The constant levels of VDAC and Hsp60 protein during the first 24 h after MOMP (Figure 5A) argues that a loss of mitochondrial mass is not the immediate cause of ATP depletion. The earliest event we observed after MOMP was a loss of mitochondrial respiration (Figure 5B). Correction of the data for incomplete induction of MOMP in the cell population (Figure 5C) revealed that both basal respiration of intact cells and ADP-stimulated (phosphorylating) respiration of digitonin-permeabilized cells were almost completely inhibited within 24 h after OHT addition. Similarly, the maximal respiratory capacity of mitochondria, measured as FCCP-stimulated respiration, was almost completely lost in both intact and digitonin-permeabilized cells.

This loss of respiration precedes any other observed sign of compromised mitochondrial function (compare e.g., the slower decay of $\Delta\Psi_m$ and cellular ATP content shown in Figure 5C). Taken together, our data strongly argue that MOMP leads first to a loss of mitochondrial bioenergetic

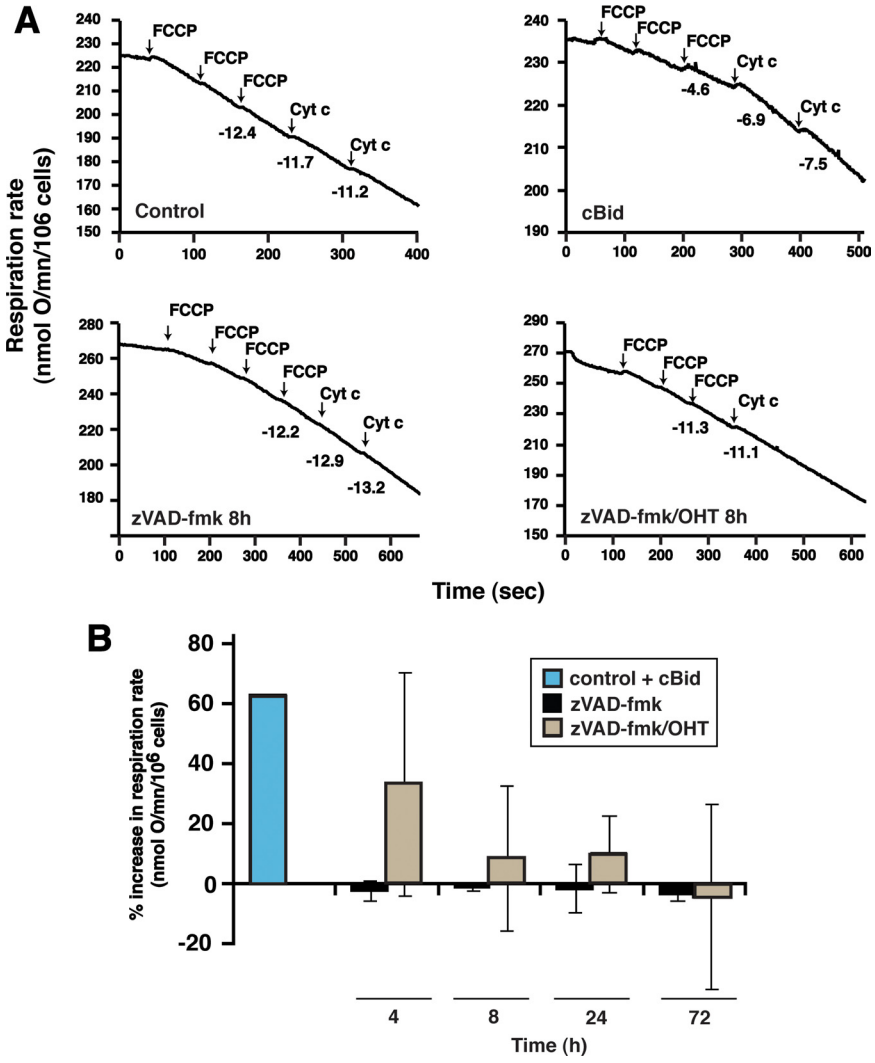

Figure 6. Exogenous cytochrome c failed to reverse inhibition of respiratory function caused by MOMP. 293T BimS-ER/GFP cells were collected at various time points after treatment with vehicle (control), zVAD-fmk, or OHT plus zVAD-fmk. Cells were then treated with a low concentration of digitonin to permeabilize the plasma membrane, while the mitochondrial membranes remained intact (see *Materials and Methods*). (A) Representative oxygen consumption curves. Maximal respiration (in the presence of glutamate/malate and FCCP) was followed before and after the addition of exogenous cytochrome c in control, zVAD, or zVAD/OHT-treated digitonin-permeabilized cells. As a positive control, N/C-Bid (14 nM) was added to a separate sample of zVAD-treated cells 30 min after digitonin incubation. Numbers under the curves indicate respiratory rates (nmol O_2/min/10^6 cells). As expected, respiration in the control cells was not stimulated by exogenous cytochrome c, as MOMs were intact. In contrast, N/C-Bid caused permeabilization of the MOM, and exogenous cytochrome c was therefore able to gain access to respiratory complexes to stimulate respiration. (B) Summary of effects of cytochrome c on respiration, expressed as a percentage of the maximal increase expected, based on the measured percentage of cells having undergone MOMP. Exogenous cytochrome c partially restored respiration 4 h after OHT addition, but not at later times. Data show the average change in the rate of maximal respiration after addition of exogenous cytochrome c, measured 4, 8, 24, and 72 h after zVAD/OHT treatment. Error bars, SD from three to five independent experiments.

function and later a gradual decline in cellular ATP. This depletion of ATP and presumably other NTP pools would likely account for the observed gradual slowdown in DNA synthesis and eventual proliferation arrest.

As mentioned earlier, previous experiments suggested that initially after MOMP, mitochondria function adequately in cytochrome c–dependent respiration. Later, however, cytoplasmic holocytochrome c concentrations may be reduced because of degradation (see *Discussion*). To determine whether cytochrome c loss could be solely responsible for bioenergetic failure, we tested whether adding exogenous cytochrome c to cells permeabilized after MOMP could restore mitochondrial respiratory activity (Figure 6). First, we confirmed that mitochondria within permeabilized nonapoptotic cells incubated with cBid protein released cytochrome c, and the resulting loss of respiration was reversed upon addition of exogenous cytochrome c. In contrast, when we permeabilized cells as early as 4 h after induction of BimS-ER by OHT, in the presence of Q-VD, respiration could only be partially restored by exogenous cytochrome c, and at 8 h, exogenous cytochrome c had almost no effect (Figure 6). Thus, the respiration defect had to involve an additional mechanism other than loss of cytochrome c. This loss of cytochrome c–stimulated respiratory function occurred early after OHT addition and may be the earliest cause of cell death when caspases are inactive.

We then evaluated respiratory rates of Q-VD– and Q-VD/OHT–treated cells that were digitonin-permeabilized and incubated with glutamate plus malate, succinate, and TMPD plus ascorbate, the substrates for complex I, complex II, and complex IV, respectively (Supplemental Figures S2 and S3; not shown). BimS-ER–induced MOMP decreased the rate of oxygen consumption via both glutamate/malate and succinate by 40–50%. Thus, within 8 h, MOMP led to a substantial loss of respiratory capacity. To identify specific defects, we measured enzyme activities of individual respiratory complexes (Figure 5E). Enzymatic activities were normalized to an invariant mitochondrial internal control, citrate synthase (CS). By correcting the data for the percentage of cells in the population that had undergone MOMP, we inferred that Complex I activity was completely lost, and COX activity was reduced by ~70% within 8 h after MOMP (compare the effects of Rotenone and KCN, specific inhibitors of Complex I and COX, respectively), whereas Complex II was unaffected. Taken together, our data point to a functional loss of specific respiratory complexes, occurring ~4–8 h after MOMP, as an early event explaining the subsequent bioenergetic decline in these cells. The apparent increase in

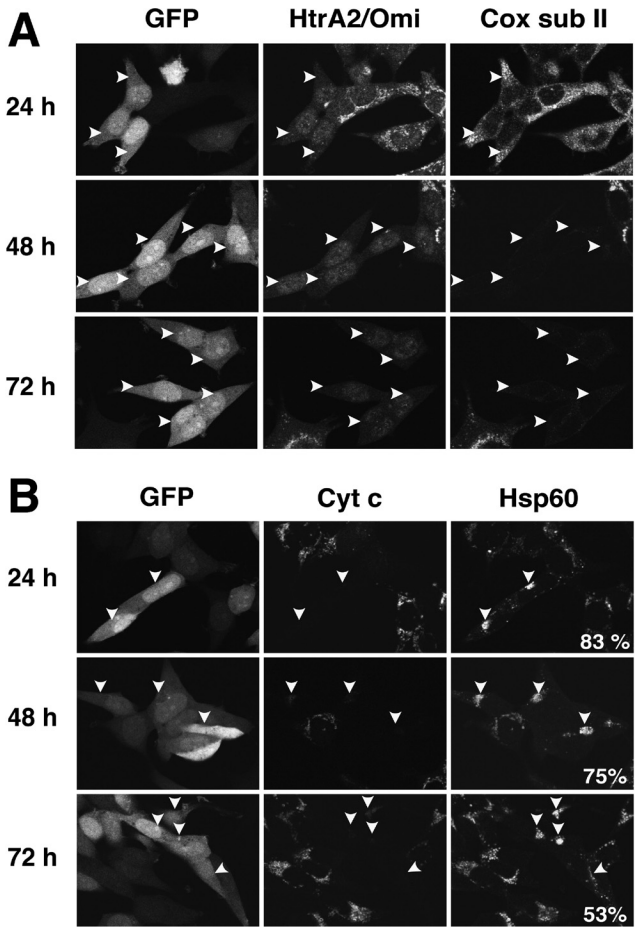

Figure 7. Directly-induced MOMP resulted in a delayed loss of mitochondrial proteins at different rates. (A) MOMP results in a loss of cytochrome c oxidase subunit II. At the indicated times after OHT addition, cells were fixed and coimmunostained for HtrA2/Omi and mitochondria-encoded cytochrome c oxidase subunit II. (B) Cells undergoing MOMP maintained some content of the mitochondrial matrix protein Hsp60 even at 72 h. Cells were treated as in A but coimmunostained for cytochrome c and Hsp60. The percentage of cells that had released cytochrome c but contained Hsp60 is shown at the bottom right of the right-most column.

Complex II activity in Figure 5E was not statistically significant.

Delayed Caspase-independent Loss of Multiple Mitochondrial Proteins Late after MOMP

Cellular levels of the mitochondrial proteins VDAC and Hsp60 remained constant for at least 24 h (Figure 5A). To examine the impact of MOMP on mitochondria at later times, we used immunofluorescence confocal microscopy to analyze proteins encoded both by nuclear genes (Complex I subunit 20 kDa [CI sub20]) and by the mitochondrial genome (cytochrome c oxidase subunit II [Cox subII]). At 24 h after OHT addition, CI sub20 and Cox subII were clearly present in cells that had undergone MOMP. However, at 48 and 72 h, these proteins were no longer detectable (Figure 7 and Supplemental Figure S1A). Cytochrome c oxidase subunit IV (Cox subIV), AIF, endoG (all nuclear-encoded), and cytochrome c oxidase subunit I (Cox subI, mitochondrial-encoded) were similarly lost at late time points (data not shown). Therefore, much after the early loss of $\Delta\Psi_m$ and OxPhos function produced by MOMP, cells also displayed a profound depletion of essential mitochondrial proteins, suggesting that MOMP led to progressive and presumably irrecoverable damage to the organelles.

Chemical Inhibition of Mitochondrial, But Not Glycolytic Functions, Caused an Immediate Arrest of Cellular Proliferation

To gauge the importance of mitochondrial bioenergetic function (OxPhos) for proliferation in the cells used in this study, we tested the effects of metabolic inhibitors (Figure 8). The uncoupler CCCP induced complete mitochondrial depolarization in 293T cells at 5 μM and profoundly inhibited cell division. Rotenone and oligomycin, which inhibit Complexes I and V (ATP synthase), respectively, also blocked proliferation. In each case, there was no decrease in cell number, and analysis with trypan blue uptake showed that none of these compounds caused cell death over the course of the experiment (not shown).

CCCP and rotenone cause loss of both ATP synthesis and $\Delta\Psi_m$. Oligomycin, however, blocks ATP synthesis without dissipating $\Delta\Psi_m$, and so we can conclude that mitochondrial ATP synthesis is required for cell proliferation. However, we cannot rule out an additional requirement for $\Delta\Psi_m$. Indeed, we would expect $\Delta\Psi_m$ to be necessary for cell survival in the long-term, as there are critical cell functions, including portions of the TCA cycle and steroid biosynthesis, that involve nuclear-encoded mitochondrial proteins. Mitochondrial import of these proteins would require an intact $\Delta\Psi_m$. (We also note that, as oligomycin had no effect on $\Delta\Psi_m$, the membrane potential after MOMP was not generated by ATP synthase acting in reverse, but rather through respiration.)

In comparison, removing glucose or adding 2-deoxyglucose, a nonmetabolyzable glucose analog, surprisingly had a negligible effect on cell proliferation (Figure 8B), as long as a mitochondrial metabolite such as glutamine was present in the medium. Even after cells had undergone MOMP, glycolysis inhibition had little effect on the timing of delayed proliferation slowdown, although there was some reduction in cell numbers, suggesting that glycolysis may help keep cells alive after MOMP (Figure 9). Based on all our data, we conclude that mitochondrial OxPhos is critically important for proliferation of these cells and, moreover, that the cause of cell death in the absence of executioner caspase activity is a loss of specific respiratory complexes occurring several hours after MOMP, followed much later by the disappearance of multiple mitochondrial proteins.

DISCUSSION

Ordinarily, a cell undergoing the "intrinsic" or mitochondrial apoptotic pathway displays the typical caspase-dependent features of apoptosis, such as nuclear fragmentation. Caspase-deficient cells undergoing MOMP do not undergo these events, but are nevertheless doomed (Xiang *et al.*, 1996; McCarthy *et al.*, 1997; Amarante-Mendes *et al.*, 1998; Hakem *et al.*, 1998; Chautan *et al.*, 1999; Haraguchi *et al.*, 2000; Vandenabeele *et al.*, 2006). Thus, MOMP ordinarily represents a point of no return for cell death. One notable exception to this is the situation of caspase inhibition (either by chemical inhibitors such as zVAD or Q-VD, or in cells genetically deficient for the Apaf-1/Caspase-9 pathway) combined with the enforced expression of GAPDH (Colell *et al.*, 2007).

We showed that cells that had engaged the mitochondrial pathway of apoptosis and lost MOM integrity were nevertheless able to synthesize DNA for at least 48 h, provided

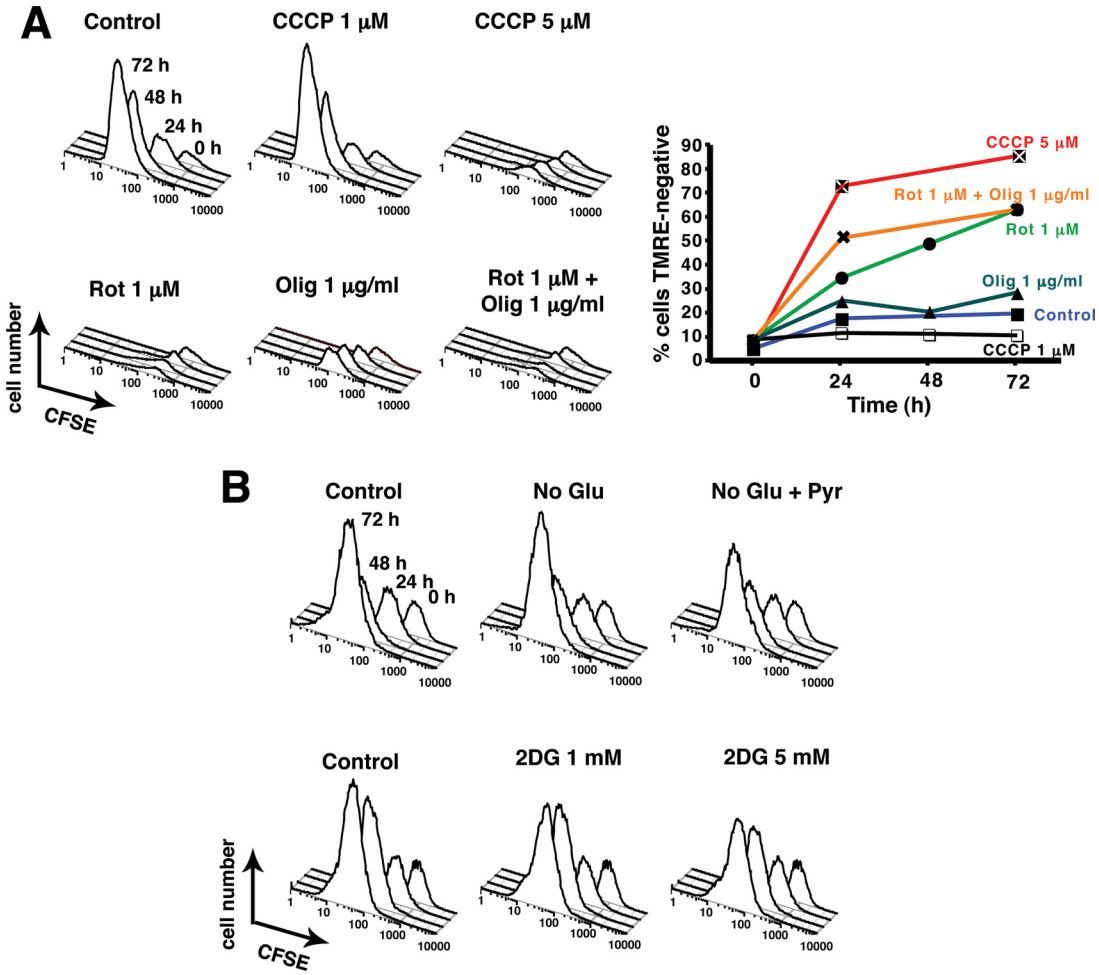

Figure 8. Blocking mitochondrial, but not glycolytic, function resulted in an immediate arrest of cellular proliferation. (A) CCCP, rotenone, and oligomycin halt proliferation immediately. Twenty-four hours after CFSE staining, 293T cells were incubated with vehicle or CCCP (1 or 5 μM), rotenone (1 μM), oligomycin (1 μg/ml), or both rotenone (1 μM) and oligomycin (1 μg/ml). Cell proliferation and $\Delta\Psi_m$ loss were monitored by CFSE fluorescence intensity (left panel) and TMRE staining (right panel), respectively, using flow cytometry. Note that oligomycin by itself did not dissipate $\Delta\Psi_m$ but nevertheless blocked cellular proliferation. (B) Inhibition of glycolysis had no effect on cell proliferation over 72 h. CFSE-stained cells were cultured either in DMEM deprived of glucose, in the presence or absence of additional sodium pyruvate (1 mM) or in regular DMEM with or without addition of 1 or 5 mM of 2-deoxyglucose. Cell proliferation was monitored by CFSE fluorescence intensity using flow cytometry.

that caspases remained inactive. Unexpectedly, the entire process of cell division was unaffected by MOMP for ~48 h. BimS-ER–expressing cells were able to complete about two rounds of cell division before their DNA replication rates gradually slowed, finally coming to a halt. From our data, we concluded that the underlying cause for this is a delayed

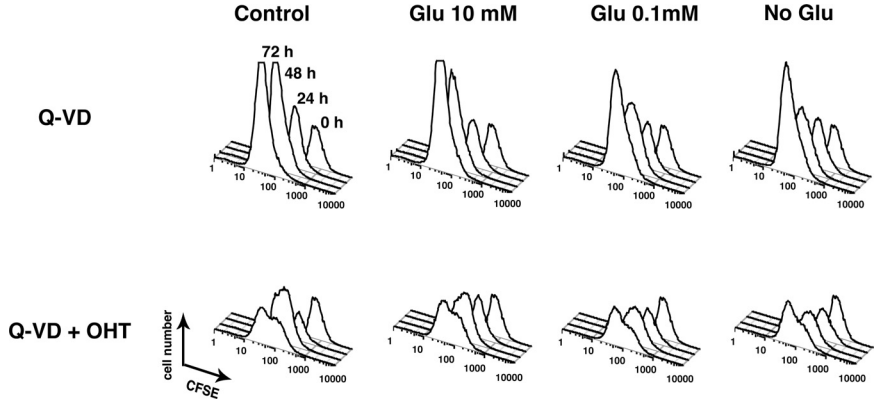

Figure 9. Removing glucose after MOMP reduced cell accumulation, but did not alter the timing of cell cycle arrest. CFSE-stained BimS-ER/DsRed2–expressing cells were cultured with or without OHT in the presence of Q-VD-fmk for 8, 24, 48, and 72 h. (A) Eight hours after OHT addition, regular DMEM (25 mM glucose) was replaced by DMEM containing either 0, 0.1, 10 or 25 mM glucose. Cell proliferation was monitored by CFSE fluorescence intensity using flow cytometry. Similar results were obtained with the addition of 2-deoxyglucose to regular DMEM (not shown).

loss of mitochondrial function that occurs within 8 h after MOMP; this leads to a gradual depletion of cellular ATP (Figures 4 and 5).

This substantial delay in the effects of MOMP is inconsistent with the "gain of death function" hypothesis, which proposes that molecules released from mitochondria have a caspase-independent direct cytotoxic effect. In particular, we did not detect the translocation of AIF and endoG into the nucleus, consistent with earlier reports describing that AIF and endoG release are late caspase-dependent events in apoptosis (Cande *et al.,* 2004; Lakhani *et al.,* 2006). HtrA2/Omi protein, on the other hand, was released into the cytoplasm simultaneously with cytochrome c after OHT addition. HtrA2/Omi was reported to have some caspase-independent activity through its PDZ domain (Hegde *et al.,* 2002), and thus in principle, the effects we observed after MOMP could have been caused by Omi's caspase-independent function. However, Omi/Htra2 is rapidly degraded after its release from mitochondria (Sun *et al.,* 2004). In any case, it seems unlikely that Omi or other proteins released from mitochondria could be responsible for the observed gradual slowdown in DNA replication and delayed loss of proliferative capacity, especially because the impairment of mitochondrial bioenergetic function is clearly sufficient to explain these events.

In normal apoptosis, caspase cleavage of a subunit of Complex I contributes to the characteristic collapse of $\Delta\Psi_m$ and ATP production after MOMP (Ricci *et al.,* 2004). Here we show that, even in absence of caspase activation, Complex I and COX activities became impaired. However, these defects were not seen immediately after MOMP, but began to develop within ~4 h and were strongly evident at 8 h, when we observed ~100 and 70% inhibition of complexes I and IV, respectively.

Likely as a result of this substantial respiratory deficit, cellular ATP content declined slowly after MOMP, with kinetics that parallel the observed slowing in DNA synthesis. Furthermore, we showed that complete pharmacological inhibition of mitochondrial OxPhos was sufficient to block proliferation immediately, whereas blocking glycolysis had no short-term effect. The simplest explanation is that a profound loss of mitochondrial bioenergetic function is responsible for the slowing of DNA synthesis and the eventual block to cell division that we observed. However, it is conceivable that the loss of other critical mitochondrial functions also contributes to proliferative arrest.

Possible Mechanisms of the Loss of Mitochondrial Function

Cytochrome c, even after its release into the cytoplasm, has been shown to be abundant enough to sustain respiration (Waterhouse *et al.,* 2001; Ricci *et al.,* 2004). Nevertheless, we can hypothesize that over time the pool of cytoplasmic holocytochrome c is depleted through degradation, perhaps by proteasomes (Cozzolino *et al.,* 2004). We would not expect the pool of holocytochrome c to be replenishable by de novo synthesis if the barrier function of the MOM is compromised. This is because the enzyme heme lyase covalently attaches the heme group to apocytochrome c inside the IMS (Enosawa and Ohashi, 1986; Dumont *et al.,* 1988; Nicholson *et al.,* 1988; Stuart and Neupert, 1990), and MOMP would prevent the accumulation of newly synthesized apocytochrome c in the IMS. However, addition of exogenous cytochrome c did not significantly restore normal oxygen consumption rates in cells permeabilized after MOMP, even as early as 8 h after OHT treatment (Figure 6). We conclude that the MOMP-induced impairment in mitochondrial OxPhos function in cells treated with OHT plus zVAD-fmk cannot be explained simply by a loss of cytochrome c.

Rather, we found that MOMP in the absence of caspase activation led to dysfunction of specific respiratory complexes: within 8 h we saw nearly the complete loss of Complex I activity and a partial deficiency of Complex IV, at a time when 80% of the cells maintained $\Delta\Psi$m. Complex II function remained unaffected. Possibly, the presence of intact Complex II activity along with a partially functional Complex IV (~30% of normal activity) is sufficient to allow a low level of electron transport activity, assuming that complex III (which for technical reasons was not assayed here) also remains entirely or partly intact. Indeed, a previous study showed that it was possible to inhibit the activity of various OxPhos complexes, up to a critical value, without affecting the rate of mitochondrial respiration or ATP synthesis (Rossignol *et al.,* 2003). This may explain why ATP and mitochondrial $\Delta\Psi_m$ are lost only gradually after MOMP. However, we presume that the respiratory short-cut involving complexes II and IV remains active only temporarily, as eventually mitochondria underwent serious degradative effects (Figure 7; not shown).

While our work was ongoing, others reported that in caspase-inhibited cells after MOMP, or in isolated mitochondria in which the MOM is disrupted via the permeability transition, Tim23 is degraded by intramitochondrial proteases, in a manner unrelated to autophagy (Goemans *et al.,* 2008). These authors also speculated that the MOMP-induced loss of an IMS protein, DPP1/Timm8a (Arnoult *et al.,* 2005), which is associated with Tim23 and aids in the proper folding of that protein, may lead to Tim23 degradation.

Consistent with that prior study, we observed that by 24 h after MOMP, mitochondria had indeed lost Tim23 (Supplemental Figure S5). However, at 8 h, half of the cells that had undergone MOMP still displayed mitochondrial localization of Tim23. By that time, cells had completely lost Complex I activity, suggesting that the loss of respiratory function preceded loss of Tim23. Moreover, although cells that lose Tim23 would immediately suffer a loss of mitochondrial protein import, the resulting depletion of preexisting mitochondrial proteins could occur more slowly, depending on their half-life. For example, nuclear-encoded Complex II and Citrate Synthase activities remained unchanged at 24 h after MOMP induction, as did the levels of several other proteins (VDAC, AIF, endoG, HSP60; Figures 3, 5A, and 7, data not shown).

To explain the comparatively early loss of respiratory function, we hypothesize that one or more subunits of Complex I and IV are specifically degraded as a consequence of the loss of MOM integrity. One interesting possibility is that mitochondrial proteases of the AAA family might mediate degradation (Guzelin *et al.,* 1996; Arlt *et al.,* 1998; Arnold and Langer, 2002). In particular, earlier studies in yeast showed that cells deficient in cytochrome c exhibit degradation of specific subunits of cytochrome oxidase, via the AAA protease Yme1p (Pearce and Sherman, 1995).

Other mechanisms for the impairment of individual respiratory complexes are also possible. Interestingly, for example, cells underwent a partial depletion of mtDNA that paralleled the loss of respiratory function (Supplemental Figure S4). It is possible that a partial depletion of mtDNA (through an unknown mechanism) could help explain the deficiencies in complex I and COX activities, as these two complexes contain catalytic subunits encoded by mtDNA (Asin-Cayuela and Gustafsson, 2007). Similarly, there could be a reduction in the rate of mitochondrial transcription and translation.

How Could Cells Recover from Extensive Mitochondrial Deterioration?

Under unusual conditions, e.g., enforced expression of GAPDH, cells can be rescued after MOMP if caspases are inhibited (Colell *et al.,* 2007). However, the progressive deterioration of mitochondria that we observed suggests that organelles that have lost outer membrane integrity would be impossible to repair. How could the mitochondrial network recover? We hypothesize that cells must repopulate themselves with healthy mitochondria through a process of biogenesis, starting with a small remnant of undamaged mitochondria to serve as seeds. Mitochondrial fragmentation, which is typical in apoptosis, could aid cell recovery by isolating such seed mitochondria away from the damaged mitochondrial fragments, which could be eliminated by mitophagy (Elmore *et al.,* 2004; Priault *et al.,* 2005; Kim *et al.,* 2007; Twig *et al.,* 2008). The intact mitochondrial fragments would be able to divide and fuse, thereby regenerating a functional mitochondrial network.

Restoring the mitochondrial network might take quite some time. Indeed, we speculate that this is exactly what occurs over ~10 d in cells with enforced GAPDH expression (Colell *et al.,* 2007). A similar slow repopulation of cells with functional mitochondria probably occurs also in nerve growth factor (NGF)-deprived embryonic neurons cultured with caspase inhibitors, which can recover after MOMP if NGF is subsequently added back to the culture medium (Deshmukh *et al.,* 1996, 2000; Martinou *et al.,* 1999).

Cell fate in such cases may be determined by a race between the irreversible consequences of energy depletion—including mitochondrial protein degradation and the removal of damaged organelles by autophagy—and the repopulation of the cell with healthy mitochondria. At least two functions of GAPDH are required for the rescue of cells after MOMP: stimulation of glycolysis and the induction of certain autophagy genes (Colell *et al.,* 2007). It remains to be determined whether GAPDH actively promotes mitochondrial biogenesis or, by supplying energy for the cell from increased glycolysis and autophagy, simply buys more time for the cell to carry out its normal program of mitochondrial replenishment.

It is puzzling that although MOMP induced a gradual but profound depletion of cellular energy stores, this condition alone was insufficient to stimulate autophagy. Moreover, we did not detect any activation of the low energy checkpoint enzyme AMPK (not shown). In this regard, MOMP seems to produce a cellular state different from that caused by growth factor deprivation, where survival pathways such as autophagy are engaged to allow factor-deprived cells to survive indefinitely in a dormant state (Kuma *et al.,* 2004; Wullschleger *et al.,* 2006).

Requirement of Mitochondrial Bioenergetic Function for Cell Proliferation

Mitochondrial poisons, which ablate energy production completely, rapidly halted cell division (Figure 8). Thus, the substantial loss of mitochondrial ATP production by OxPhos after MOMP is most likely sufficient to cause the delayed cell cycle arrest we observed. In contrast, an inhibition of glycolysis had no immediate effect on proliferation (Figure 8). Glucose removal after MOMP caused a reduction in cell numbers (this may suggest that some cells died under these conditions), but did not alter the timing of cell proliferation arrest (Figure 9). We conclude that healthy mitochondria are essential for these cells to divide. After MOMP, glycolysis may help keep some cells alive, but appears not to be necessary for many cells to proliferate for ~48 h.

This finding may seem particularly surprising given that in tumor cells, glycolytic metabolism is often greatly enhanced (the "Warburg effect"; Gatenby and Gillies, 2004). However, even if this shift toward glycolysis occurs, it does not necessarily imply that mitochondrial metabolism is dispensable. Indeed, glycolysis accounts for at most 50–70% of total ATP production (Warburg, 1956; Moreno-Sanchez *et al.,* 2007) and often much less. One report (Zu and Guppy, 2004) concluded that, on average, the relative contribution of glycolysis to total ATP production is quite similar in normal (20%) and cancer (17%) cells.

Enhanced rates of glycolysis or glucose uptake may be important for critical metabolic pathways other than ATP synthesis (extensively reviewed by Vander Heiden *et al.,* 2009), in particular, the production of intermediate metabolites and reducing equivalents required for the biosynthesis of proteins, fatty acids, and nucleotides, which are essential for sustained tumor growth (Medes *et al.,* 1953; Ookhtens *et al.,* 1984; Homem de Bittencourt *et al.,* 1993; Kuhajda, 2000; Pfeiffer *et al.,* 2001; Bauer and Patterson, 2005; Hatzivassiliou *et al.,* 2005). Fatty acid synthesis depends also on citrate, produced in the mitochondrial matrix (Kuhajda, 2000; Hatzivassiliou *et al.,* 2005; Bui and Thompson, 2006). Thus an intriguing possibility is that mitochondrial dysfunction could impair de novo lipogenesis in tumor cells and thereby compromise cell proliferation.

Consistent with our data, mitochondrial bioenergetic function has been found indispensable for cell cycle progression in several tumor cell lines, at least under normal culture conditions. In particular, impairing mitochondrial energy production in HL-60, HeLa, or AS-30D cells using glutamine deprivation or treatment with oligomycin or rotenone results in an immediate block of cell proliferation (Sweet and Singh, 1995; Barrientos and Moraes, 1999; Armstrong *et al.,* 2001; Rodriguez-Enriquez *et al.,* 2006). In contrast, glycolytic blockers have no effect on the ability of HeLa and AS-30D cells to complete a round of cell division (Rodriguez-Enriquez *et al.,* 2006). These studies, as well as our own, emphasize that mitochondrial bioenergetic function can be critical for proliferation, even in tumor cells.

In conclusion, our data show that the intrinsic pathway of apoptosis, in the absence of caspase activation, leads to a gradual deterioration of mitochondrial function and a slow depletion of cellular ATP, resulting in a proliferation arrest and, presumably, a delayed form of cell death (although over the course of our experiments, cells did not exhibit loss of plasma membrane integrity; data not shown). This caspase-independent mode of cell death occurring via the intrinsic pathway could explain why in most cells, a simple blockade of caspases does not prevent MOMP-dependent death. Furthermore, our data suggest that cancer cells, to evade mitochondria-dependent cell death, must either block MOMP by acting upstream or, alternatively, act downstream of MOMP by 1) blocking caspase activation, 2) maintaining energy supply, and 3) repopulating the cell with healthy mitochondria. Replenishment of the mitochondrial pool may require an enhancement in mitophagy and biogenesis. Clearly, these are stringent requirements, and it seems likely that survival would be more easily regulated upstream of MOMP.

ACKNOWLEDGMENTS

We are grateful to Ryan Hastie for expert technical assistance and to all our colleagues in the Newmeyer laboratory for advice and discussions. This work was supported by National Institutes of Health Grants GM50284 and GM62289 to D.D.N.

REFERENCES

Acehan, D., Jiang, X., Morgan, D. G., Heuser, J. E., Wang, X., and Akey, C. W. (2002). Three-dimensional structure of the apoptosome: implications for assembly, procaspase-9 binding, and activation. Mol. Cell *9*, 423–432.

Aleardi, A. M., Benard, G., Augereau, O., Malgat, M., Talbot, J. C., Mazat, J. P., Letellier, T., Dachary-Prigent, J., Solaini, G. C., and Rossignol, R. (2005). Gradual alteration of mitochondrial structure and function by beta-amyloids: importance of membrane viscosity changes, energy deprivation, reactive oxygen species production, and cytochrome c release. J. Bioenerg. Biomembr. *37*, 207–225.

Amarante-Mendes, G. P., Finucane, D. M., Martin, S. J., Cotter, T. G., Salvesen, G. S., and Green, D. R. (1998). Anti-apoptotic oncogenes prevent caspase-dependent and independent commitment for cell death. Cell Death Differ. *5*, 298–306.

Antonsson, B., Montessuit, S., Sanchez, B., and Martinou, J. C. (2001). Bax is present as a high molecular weight oligomer/complex in the mitochondrial membrane of apoptotic cells. J. Biol. Chem. *276*, 11615–11623.

Arlt, H., Steglich, G., Perryman, R., Guiard, B., Neupert, W., and Langer, T. (1998). The formation of respiratory chain complexes in mitochondria is under the proteolytic control of the m-AAA protease. EMBO J. *17*, 4837–4847.

Armstrong, J. S., Hornung, B., Lecane, P., Jones, D. P., and Knox, S. J. (2001). Rotenone-induced G2/M cell cycle arrest and apoptosis in a human B lymphoma cell line PW. Biochem. Biophys. Res. Commun. *289*, 973–978.

Arnold, I., and Langer, T. (2002). Membrane protein degradation by AAA proteases in mitochondria. Biochim. Biophys. Acta *1592*, 89–96.

Arnoult, D., Gaume, B., Karbowski, M., Sharpe, J. C., Cecconi, F., and Youle, R. J. (2003). Mitochondrial release of AIF and EndoG requires caspase activation downstream of Bax/Bak-mediated permeabilization. EMBO J. *22*, 4385–4399.

Arnoult, D., Rismanchi, N., Grodet, A., Roberts, R. G., Seeburg, D. P., Estaquier, J., Sheng, M., and Blackstone, C. (2005). Bax/Bak-dependent release of DDP/TIMM8a promotes Drp1-mediated mitochondrial fission and mitoptosis during programmed cell death. Curr. Biol. *15*, 2112–2118.

Asin-Cayuela, J., and Gustafsson, C. M. (2007). Mitochondrial transcription and its regulation in mammalian cells. Trends Biochem. Sci. *32*, 111–117.

Barrientos, A., and Moraes, C. T. (1999). Titrating the effects of mitochondrial complex I impairment in the cell physiology. J. Biol. Chem. *274*, 16188–16197.

Bauer, S., and Patterson, P. H. (2005). The cell cycle-apoptosis connection revisited in the adult brain. J. Cell Biol. *171*, 641–650.

Birch-Machin, M. A., Shepherd, I. M., Watmough, N. J., Sherratt, H. S., Bartlett, K., Darley-Usmar, V. M., Milligan, D. W., Welch, R. J., Aynsley-Green, A., and Turnbull, D. M. (1989). Fatal lactic acidosis in infancy with a defect of complex III of the respiratory chain. Pediatr. Res. *25*, 553–559.

Bossy-Wetzel, E., Newmeyer, D. D., and Green, D. R. (1998). Mitochondrial cytochrome c release in apoptosis occurs upstream of DEVD-specific caspase activation and independently of mitochondrial transmembrane depolarization. EMBO J. *17*, 37–49.

Brown, G. C., Nicholls, D. G., and Cooper, C. E. (1999). Mitochondria and Cell Death, Princeton, NJ: Princeton University Press, vii–viii.

Bui, T., and Thompson, C. B. (2006). Cancer's sweet tooth. Cancer Cell *9*, 419–420.

Cande, C., Vahsen, N., Garrido, C., and Kroemer, G. (2004). Apoptosis-inducing factor (AIF): caspase-independent after all. Cell Death Differ. *11*, 591–595.

Cha, K. Y., Lee, S. H., Chung, H. M., Baek, K. H., Cho, S. W., and Kwack, K. B. (2005). Quantification of mitochondrial DNA using real-time polymerase chain reaction in patients with premature ovarian failure. Fertil. Steril. *84*, 1712–1718.

Chautan, M., Chazal, G., Cecconi, F., Gruss, P., and Golstein, P. (1999). Interdigital cell death can occur through a necrotic and caspase-independent pathway. Curr. Biol. *9*, 967–970.

Colell, A., *et al*. (2007). GAPDH and autophagy preserve survival after apoptotic cytochrome c release in the absence of caspase activation. Cell *129*, 983–997.

Cozzolino, M., *et al*. (2004). Apoptosome inactivation rescues proneural and neural cells from neurodegeneration. Cell Death Differ. *11*, 1179–1191.

Deshmukh, M., Kuida, K., and Johnson, E. M., Jr. (2000). Caspase inhibition extends the commitment to neuronal death beyond cytochrome c release to the point of mitochondrial depolarization. J. Cell Biol. *150*, 131–143.

Deshmukh, M., Vasilakos, J., Deckwerth, T. L., Lampe, P. A., Shivers, B. D., and Johnson, E. M., Jr. (1996). Genetic and metabolic status of NGF-deprived sympathetic neurons saved by an inhibitor of ICE family proteases. J. Cell Biol. *135*, 1341–1354.

Dumont, M. E., Ernst, J. F., and Sherman, F. (1988). Coupling of heme attachment to import of cytochrome c into yeast mitochondria. Studies with heme lyase-deficient mitochondria and altered apocytochromes c. J. Biol. Chem. *263*, 15928–15937.

Elmore, S. P., Nishimura, Y., Qian, T., Herman, B., and Lemasters, J. J. (2004). Discrimination of depolarized from polarized mitochondria by confocal fluorescence resonance energy transfer. Arch. Biochem. Biophys. *422*, 145–152.

Enosawa, S., and Ohashi, A. (1986). Localization of enzyme for heme attachment to apocytochrome c in yeast mitochondria. Biochem. Biophys. Res. Commun. *141*, 1145–1150.

Gatenby, R. A., and Gillies, R. J. (2004). Why do cancers have high aerobic glycolysis? Nat. Rev. Cancer *4*, 891–899.

Goemans, C. G., Boya, P., Skirrow, C. J., and Tolkovsky, A. M. (2008). Intra-mitochondrial degradation of Tim23 curtails the survival of cells rescued from apoptosis by caspase inhibitors. Cell Death Differ. *15*, 545–554.

Griffiths, G. J., Dubrez, L., Morgan, C. P., Jones, N. A., Whitehouse, J., Corfe, B. M., Dive, C., and Hickman, J. A. (1999). Cell damage-induced conformational changes of the pro-apoptotic protein Bak in vivo precede the onset of apoptosis. J. Cell Biol. *144*, 903–914.

Guzelin, E., Rep, M., and Grivell, L. A. (1996). Afg3p, a mitochondrial ATP-dependent metalloprotease, is involved in degradation of mitochondrially-encoded Cox1, Cox3, Cob, Su6, Su8 and Su9 subunits of the inner membrane complexes III, IV and V. FEBS Lett. *381*, 42–46.

Hakem, R., *et al*. (1998). Differential requirement for caspase 9 in apoptotic pathways in vivo. Cell *94*, 339–352.

Haraguchi, M., Torii, S., Matsuzawa, S., Xie, Z., Kitada, S., Krajewski, S., Yoshida, H., Mak, T. W., and Reed, J. C. (2000). Apoptotic protease activating factor 1 (Apaf-1)-independent cell death suppression by Bcl-2. J. Exp. Med. *191*, 1709–1720.

Hatzivassiliou, G., Zhao, F., Bauer, D. E., Andreadis, C., Shaw, A. N., Dhanak, D., Hingorani, S. R., Tuveson, D. A., and Thompson, C. B. (2005). ATP citrate lyase inhibition can suppress tumor cell growth. Cancer Cell *8*, 311–321.

Hegde, R., *et al*. (2002). Identification of Omi/HtrA2 as a mitochondrial apoptotic serine protease that disrupts inhibitor of apoptosis protein-caspase interaction. J. Biol. Chem. *277*, 432–438.

Hoffarth, S., Zitzer, A., Wiewrodt, R., Hahnel, P. S., Beyer, V., Kreft, A., Biesterfeld, S., and Schuler, M. (2008). pp32/PHAPI determines the apoptosis response of non-small-cell lung cancer. Cell Death Differ. *15*, 161–170.

Homem de Bittencourt, P. I., Jr., Peres, C. M., Yano, M. M., Hirata, M. H., and Curi, R. (1993). Pyruvate is a lipid precursor for rat lymphocytes in culture: evidence for a lipid exporting capacity. Biochem. Mol. Biol. Int. *30*, 631–641.

Horvitz, H. R., and Sternberg, P. W. (1991). Multiple intercellular signalling systems control the development of the *Caenorhabditis elegans* vulva. Nature *351*, 535–541.

Hsu, Y. T., Wolter, K. G., and Youle, R. J. (1997). Cytosol-to-membrane redistribution of Bax and Bcl-X(L) during apoptosis. Proc. Natl. Acad. Sci. USA *94*, 3668–3672.

Hsu, Y. T., and Youle, R. J. (1997). Nonionic detergents induce dimerization among members of the Bcl-2 family. J. Biol. Chem. *272*, 13829–13834.

Janssen, K., Pohlmann, S., Janicke, R. U., Schulze-Osthoff, K., and Fischer, U. (2007). Apaf-1 and caspase-9 deficiency prevents apoptosis in a Bax-controlled pathway and promotes clonogenic survival during paclitaxel treatment. Blood *110*, 3662–3672.

Jiang, X., and Wang, X. (2000). Cytochrome c promotes caspase-9 activation by inducing nucleotide binding to Apaf-1. J. Biol. Chem. *275*, 31199–31203.

Kim, I., Rodriguez-Enriquez, S., and Lemasters, J. J. (2007). Selective degradation of mitochondria by mitophagy. Arch. Biochem. Biophys. *462*, 245–253.

Kluck, R. M., Bossy-Wetzel, E., Green, D. R., and Newmeyer, D. D. (1997). The release of cytochrome c from mitochondria: a primary site for Bcl-2 regulation of apoptosis. Science *275*, 1132–1136.

Kluck, R. M., Ellerby, L. M., Ellerby, H. M., Naiem, S., Yaffe, M. P., Margoliash, E., Bredesen, D., Mauk, A. G., Sherman, F., and Newmeyer, D. D. (2000). Determinants of cytochrome c pro-apoptotic activity. The role of lysine 72 trimethylation. J. Biol. Chem. *275*, 16127–16133.

Kuhajda, F. P. (2000). Fatty-acid synthase and human cancer: new perspectives on its role in tumor biology. Nutrition *16*, 202–208.

Kuma, A., Hatano, M., Matsui, M., Yamamoto, A., Nakaya, H., Yoshimori, T., Ohsumi, Y., Tokuhisa, T., and Mizushima, N. (2004). The role of autophagy during the early neonatal starvation period. Nature *432*, 1032–1036.

Kuwana, T., Bouchier-Hayes, L., Chipuk, J. E., Bonzon, C., Sullivan, B. A., Green, D. R., and Newmeyer, D. D. (2005). BH3 domains of BH3-only proteins differentially regulate Bax-mediated mitochondrial membrane permeabilization both directly and indirectly. Mol. Cell *17*, 525–535.

Kuwana, T., Mackey, M. R., Perkins, G., Ellisman, M. H., Latterich, M., Schneiter, R., Green, D. R., and Newmeyer, D. D. (2002). Bid, Bax, and lipids cooperate to form supramolecular openings in the outer mitochondrial membrane. Cell *111*, 331–342.

Lakhani, S. A., Masud, A., Kuida, K., Porter, G. A., Jr., Booth, C. J., Mehal, W. Z., Inayat, I., and Flavell, R. A. (2006). Caspases 3 and 7, key mediators of mitochondrial events of apoptosis. Science *311*, 847–851.

Lavrik, I. N., Golks, A., and Krammer, P. H. (2005). Caspases: pharmacological manipulation of cell death. J. Clin Invest. *115*, 2665–2672.

Li, L. Y., Luo, X., and Wang, X. (2001). Endonuclease G is an apoptotic DNase when released from mitochondria. Nature *412*, 95–99.

Liu, J. R., Opipari, A. W., Tan, L., Jiang, Y., Zhang, Y., Tang, H., and Nunez, G. (2002). Dysfunctional apoptosome activation in ovarian cancer: implications for chemoresistance. Cancer Res. *62*, 924–931.

Liu, X., Kim, C. N., Yang, J., Jemmerson, R., and Wang, X. (1996). Induction of apoptotic program in cell-free extracts: requirement for dATP and cytochrome c. Cell *86*, 147–157.

Lyons, A. B., Hasbold, J., and Hodgkin, P. D. (2001). Flow cytometric analysis of cell division history using dilution of carboxyfluorescein diacetate succinimidyl ester, a stably integrated fluorescent probe. Methods Cell Biol. *63*, 375–398.

Marani, M., Tenev, T., Hancock, D., Downward, J., and Lemoine, N. R. (2002). Identification of novel isoforms of the BH3 domain protein Bim which directly activate Bax to trigger apoptosis. Mol. Cell. Biol. *22*, 3577–3589.

Marsden, V. S., Kaufmann, T., O'Reilly, L., A., Adams, J. M., and Strasser, A. (2006). Apaf-1 and caspase-9 are required for cytokine withdrawal-induced apoptosis of mast cells but dispensable for their functional and clonogenic death. Blood *107*, 1872–1877.

Martinou, I., Desagher, S., Eskes, R., Antonsson, B., Andre, E., Fakan, S., and Martinou, J. C. (1999). The release of cytochrome c from mitochondria during apoptosis of NGF-deprived sympathetic neurons is a reversible event. J. Cell Biol. *144*, 883–889.

McCarthy, N. J., Whyte, M. K., Gilbert, C. S., and Evan, G. I. (1997). Inhibition of Ced-3/ICE-related proteases does not prevent cell death induced by oncogenes, DNA damage, or the Bcl-2 homologue Bak. J. Cell Biol. *136*, 215–227.

Medes, G., Thomas, A., and Weinhouse, S. (1953). Metabolism of neoplastic tissue. IV. A study of lipid synthesis in neoplastic tissue slices in vitro. Cancer Res. *13*, 27–29.

Milano, J., and Day, B. J. (2000). A catalytic antioxidant metalloporphyrin blocks hydrogen peroxide-induced mitochondrial DNA damage. Nucleic Acids Res. *28*, 968–973.

Moreno-Sanchez, R., Rodriguez-Enriquez, S., Marin-Hernandez, A., and Saavedra, E. (2007). Energy metabolism in tumor cells. FEBS J. *274*, 1393–1418.

Nachmias, B., Ashhab, Y., and Ben-Yehuda, D. (2004). The inhibitor of apoptosis protein family (IAPs): an emerging therapeutic target in cancer. Semin. Cancer Biol. *14*, 231–243.

Newmeyer, D. D., Farschon, D. M., and Reed, J. C. (1994). Cell-free apoptosis in *Xenopus* egg extracts: inhibition by Bcl-2 and requirement for an organelle fraction enriched in mitochondria. Cell *79*, 353–364.

Nicholson, D. W. (1999). Caspase structure, proteolytic substrates, and function during apoptotic cell death. Cell Death Differ. *6*, 1028–1042.

Nicholson, D. W., Hergersberg, C., and Neupert, W. (1988). Role of cytochrome c heme lyase in the import of cytochrome c into mitochondria. J. Biol. Chem. *263*, 19034–19042.

Ookhtens, M., Kannan, R., Lyon, I., and Baker, N. (1984). Liver and adipose tissue contributions to newly formed fatty acids in an ascites tumor. Am J. Physiol. *247*, R146–R153.

Pearce, D. A., and Sherman, F. (1995). Degradation of cytochrome oxidase subunits in mutants of yeast lacking cytochrome c and suppression of the degradation by mutation of yme1. J. Biol. Chem. *270*, 20879–20882.

Pfeiffer, T., Schuster, S., and Bonhoeffer, S. (2001). Cooperation and competition in the evolution of ATP-producing pathways. Science *292*, 504–507.

Philchenkov, A., Zavelevich, M., Kroczak, T. J., and Los, M. (2004). Caspases and cancer: mechanisms of inactivation and new treatment modalities. Exp. Oncol. *26*, 82–97.

Priault, M., Salin, B., Schaeffer, J., Vallette, F. M., di Rago, J. P., and Martinou, J. C. (2005). Impairing the bioenergetic status and the biogenesis of mitochondria triggers mitophagy in yeast. Cell Death Differ. *12*, 1613–1621.

Ricci, J. E., Munoz-Pinedo, C., Fitzgerald, P., Bailly-Maitre, B., Perkins, G. A., Yadava, N., Scheffler, I. E., Ellisman, M. H., and Green, D. R. (2004). Disruption of mitochondrial function during apoptosis is mediated by caspase cleavage of the p75 subunit of complex I of the electron transport chain. Cell *117*, 773–786.

Rodriguez-Enriquez, S., Vital-Gonzalez, P. A., Flores-Rodriguez, F. L., Marin-Hernandez, A., Ruiz-Azuara, L., and Moreno-Sanchez, R. (2006). Control of cellular proliferation by modulation of oxidative phosphorylation in human and rodent fast-growing tumor cells. Toxicol. Appl. Pharmacol. *215*, 208–217.

Rossignol, R., Faustin, B., Rocher, C., Malgat, M., Mazat, J. P., and Letellier, T. (2003). Mitochondrial threshold effects. Biochem. J. *370*, 751–762.

Savill, J., and Fadok, V. (2000). Corpse clearance defines the meaning of cell death. Nature *407*, 784–788.

Slee, E. A., *et al*. (1999). Ordering the cytochrome c-initiated caspase cascade: hierarchical activation of caspases-2, -3, -6, -7, -8, and -10 in a caspase-9-dependent manner. J. Cell Biol. *144*, 281–292.

Soengas, M. S., *et al.* (2001). Inactivation of the apoptosis effector Apaf-1 in malignant melanoma. Nature *409*, 207–211.

Stuart, R. A., and Neupert, W. (1990). Apocytochrome c: an exceptional mitochondrial precursor protein using an exceptional import pathway. Biochimie *72*, 115–121.

Sun, X. M., Butterworth, M., MacFarlane, M., Dubiel, W., Ciechanover, A., and Cohen, G. M. (2004). Caspase activation inhibits proteasome function during apoptosis. Mol. Cell *14*, 81–93.

Susin, S. A., *et al.* (1999). Molecular characterization of mitochondrial apoptosis-inducing factor. Nature *397*, 441–446.

Sweet, S., and Singh, G. (1995). Accumulation of human promyelocytic leukemic (HL-60) cells at two energetic cell cycle checkpoints. Cancer Res. *55*, 5164–5167.

Taylor, R. C., Cullen, S. P., and Martin, S. J. (2007). Apoptosis: controlled demolition at the cellular level. Nat. Rev. Mol. Cell Biol. *9*, 231–241.

Twig, G., *et al.* (2008). Fission and selective fusion govern mitochondrial segregation and elimination by autophagy. EMBO J. *27*, 433–446.

Vandenabeele, P., Vanden Berghe, T., and Festjens, N. (2006). Caspase inhibitors promote alternative cell death pathways. Sci. STKE *2006*, pe44.

Vander Heiden, M. G., Cantley, L. C., and Thompson, C. B. (2009). Understanding the Warburg effect: the metabolic requirements of cell proliferation. Science *324*, 1029–1033.

Vaux, D. L., and Korsmeyer, S. J. (1999). Cell death in development. Cell *96*, 245–254.

von Ahsen, O., Renken, C., Perkins, G., Kluck, R. M., Bossy-Wetzel, E., and Newmeyer, D. D. (2000). Preservation of mitochondrial structure and function after Bid- or Bax-mediated cytochrome c release. J. Cell Biol. *150*, 1027–1036.

Wang, X. (2001). The expanding role of mitochondria in apoptosis. Genes Dev. *15*, 2922–2933.

Warburg, O. (1956). On the origin of cancer cells. Science *123*, 309–314.

Waterhouse, N. J., Goldstein, J. C., von Ahsen, O., Schuler, M., Newmeyer, D. D., and Green, D. R. (2001). Cytochrome c maintains mitochondrial transmembrane potential and ATP generation after outer mitochondrial membrane permeabilization during the apoptotic process. J. Cell Biol. *153*, 319–328.

Wei, M. C., Lindsten, T., Mootha, V. K., Weiler, S., Gross, A., Ashiya, M., Thompson, C. B., and Korsmeyer, S. J. (2000). tBID, a membrane-targeted death ligand, oligomerizes BAK to release cytochrome c. Genes Dev. *14*, 2060–2071.

Wei, M. C., Zong, W. X., Cheng, E. H., Lindsten, T., Panoutsakopoulou, V., Ross, A. J., Roth, K. A., MacGregor, G. R., Thompson, C. B., and Korsmeyer, S. J. (2001). Proapoptotic BAX and BAK: a requisite gateway to mitochondrial dysfunction and death. Science *292*, 727–730.

Wharton, B. A., and Tzagoloff, A. (1967). Cytochrome oxidase from beef heart mitochondria. Methods Enzymol. *10*, 245–250.

Wolter, K. G., Hsu, Y. T., Smith, C. L., Nechushtan, A., Xi, X. G., and Youle, R. J. (1997). Movement of Bax from the cytosol to mitochondria during apoptosis. J. Cell Biol. *139*, 1281–1292.

Wullschleger, S., Loewith, R., and Hall, M. N. (2006). TOR signaling in growth and metabolism. Cell *124*, 471–484.

Xiang, J., Chao, D. T., and Korsmeyer, S. J. (1996). BAX-induced cell death may not require interleukin 1 beta-converting enzyme-like proteases. Proc. Natl. Acad. Sci. USA *93*, 14559–14563.

Zu, X. L., and Guppy, M. (2004). Cancer metabolism: facts, fantasy, and fiction. Biochem. Biophys. Res. Commun. *313*, 459–465.